Electronic supplement to:

Crustal characteristics in the subduction zone of Mexico: implication of the tectonostratigraphic terranes on slab tearing

D. Carciumaru[1], R. Ortega[1], J. Castillo Castellanos[2] and E. Huesca–Perez[3]

[1]Centro de Investigación Científica y de Educación Superior
de Ensenada, Unidad La Paz. Miraflores 334. Col. Bellavista.,
23050, La Paz, BCS, México, e-mail: ortega@cicese.mx

[2]Seismological Laboratory, Department of Earth and Planetary Sciences, California Institute of Technology, Pasadena, CA, USA

[3]CONACYT - Centro de Investigación Científica y de Educación Superior
de Ensenada, Unidad La Paz. Miraflores 334. Col. Bellavista.,
23050, La Paz, BCS, México

In figure S1 we show the iso-contours depth of Pardo and Suarez (1995) and the same features of Figure 1. Note the smooth shape of the subducting slab if compared with the figure 6.

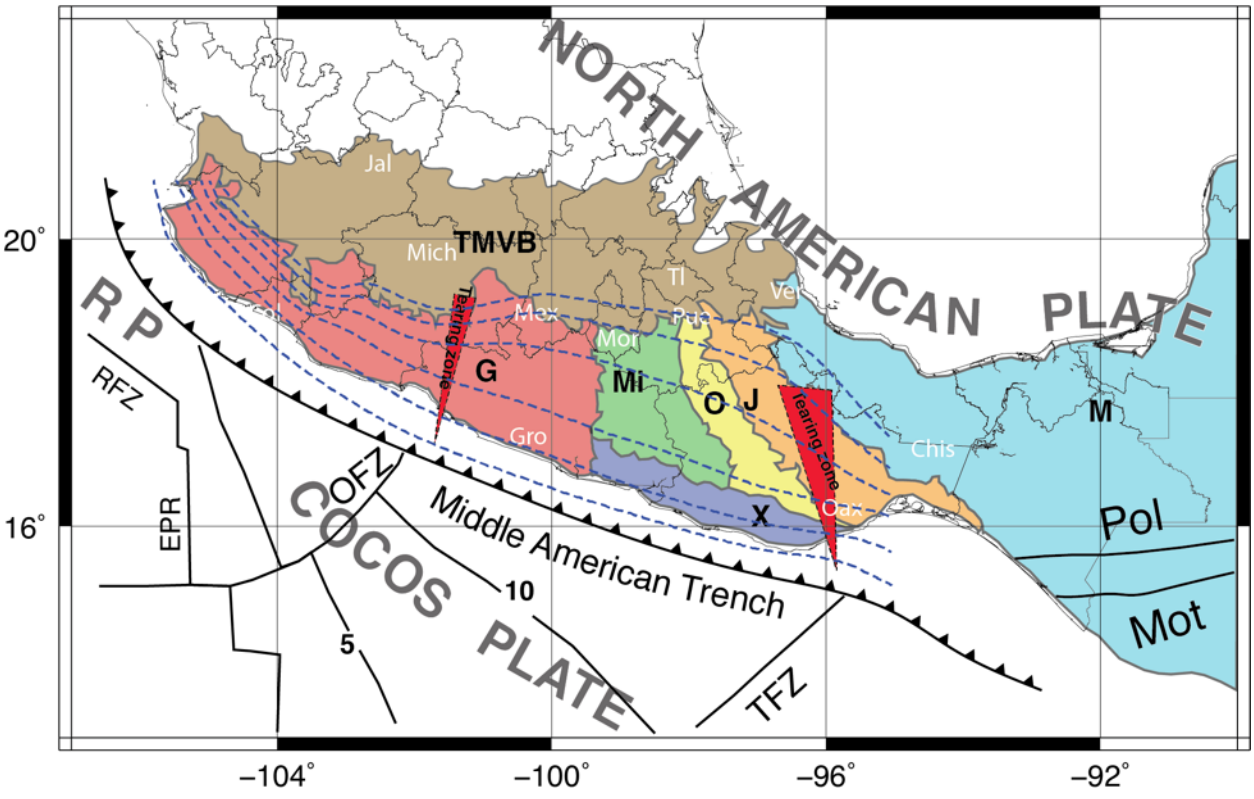

Figure S1. Tectonostratigraphic terranes of the subduction in Mexico after Campa and Coney (1983). TMB- Trans Mexican Volcanic Belt, G- Guerrero, Mi- Mixteca, O- Oaxaca, J- Juarez, X- Xolapa, M- Maya. Faults and fracture zones: RFZ- Rivera Fracture Zone, EPR- East Pacific Rise, TFZ -Tehuantepec Fracture Zone, OFZ- Orozco Fracture Zone, Pol- Polochic Fault, Mot- Motagua Fault, RP- Rivera plate. The numbers represent the age of the plate in Ma from magnetic anomalies in the ocean floor. Political borders in this region of Mexico are Jal- Jalisco, Mich- Michoacan, Mex- Mexico, Gro- Guerrero, Oax- Oaxaca, Chis- Chiapas, Tl- Tlaxcala, Pue- Puebla, Ver- Veracruz, Mor-Morelos.

Table S1 (Table_S1.csv) includes the moment tensor result with the six components of the 43 moment tensors (m11,m22,m33,m12,m13,m23m), the eigenvalues and eigenvectors (S, $\hat{e}$), also we present the scalar moment and eigenvalues of the deviatoric part. In addition, we present the strike, dip and rake if the principal planes, the trend and plunge of the P and T axis and the moment magnitude and focal depth.

The figures S2 to S44 are the time domain waveform inversions of each earthquake of table S1, continue lines represent observed and dashed lines are predicted.

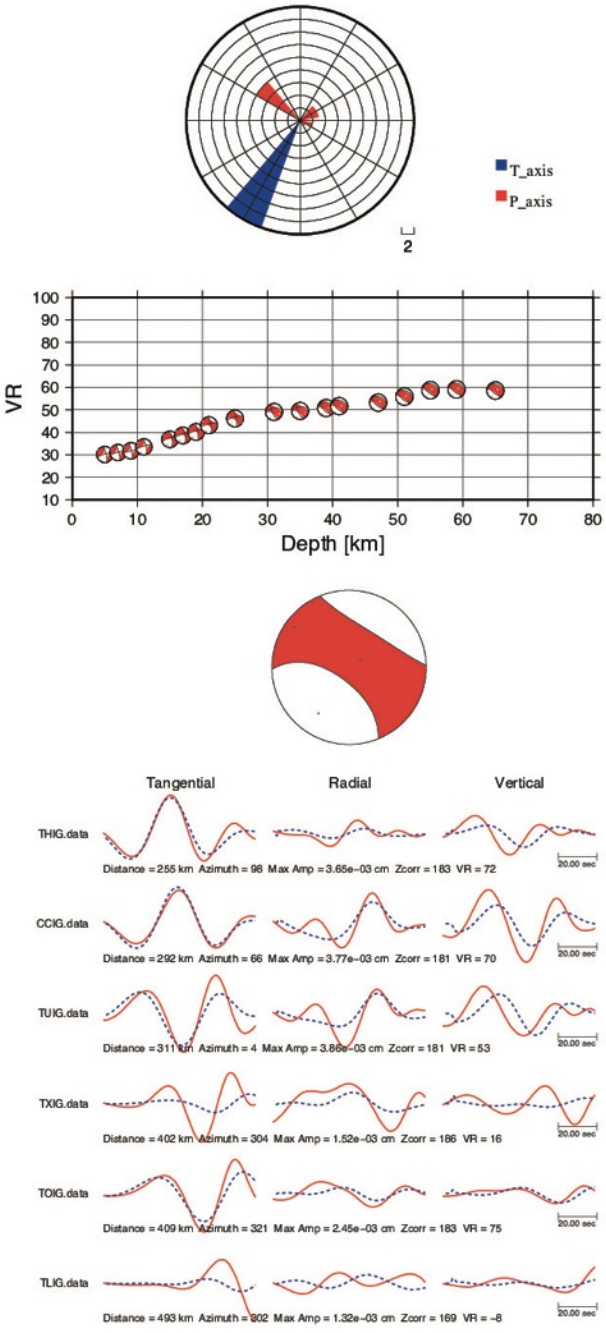

Figure S2.Moment tensor inversion of earthquake 1 (Table S1) after depth analysis. At the top we present the histogram of P and T axis. Middle. Variance Reduction (VR) as a function of depth. Bottom, time domain waveform inversion of the best solution.

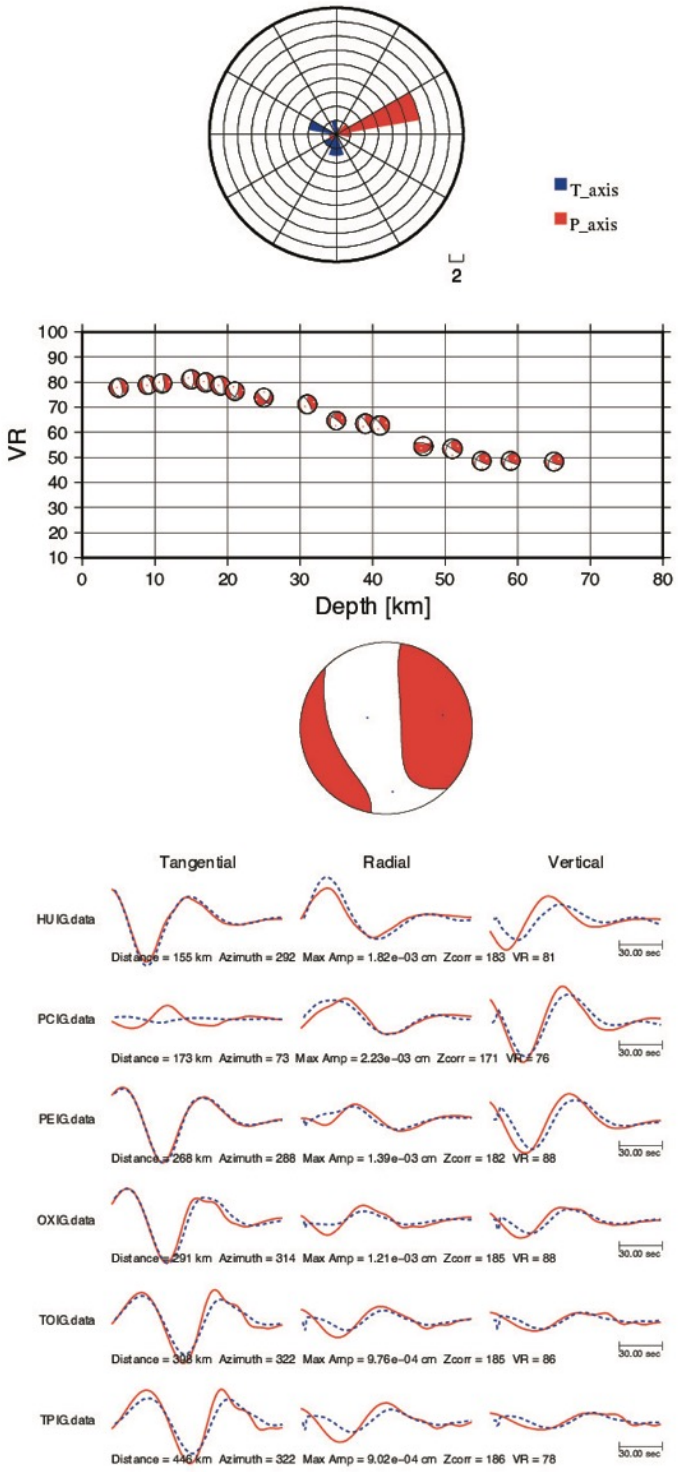

Figure S3. Moment tensor inversion of earthquake 2 (Table S1) after depth analysis. At the top we present the histogram of P and T axis. Middle. Variance Reduction (VR) as a function of depth. Bottom, time domain waveform inversion of the best solution.

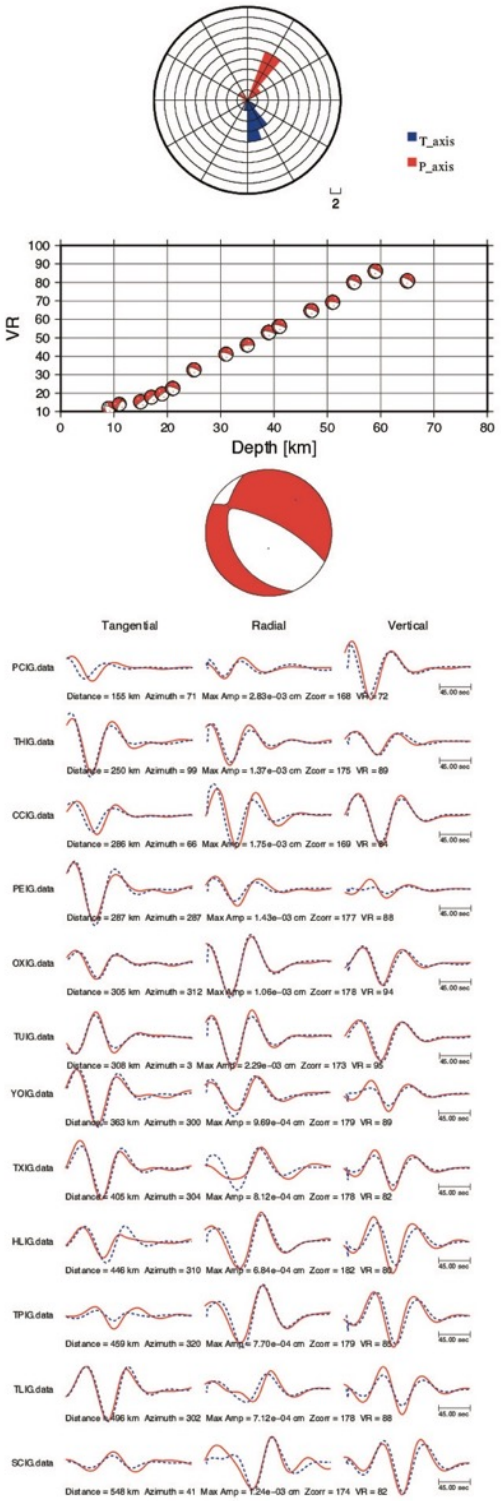

Figure S4. Moment tensor inversion of earthquake 3 (Table S1) after depth analysis. At the top we present the histogram of P and T axis. Middle. Variance Reduction (VR) as a function of depth. Bottom, time domain waveform inversion of the best solution.

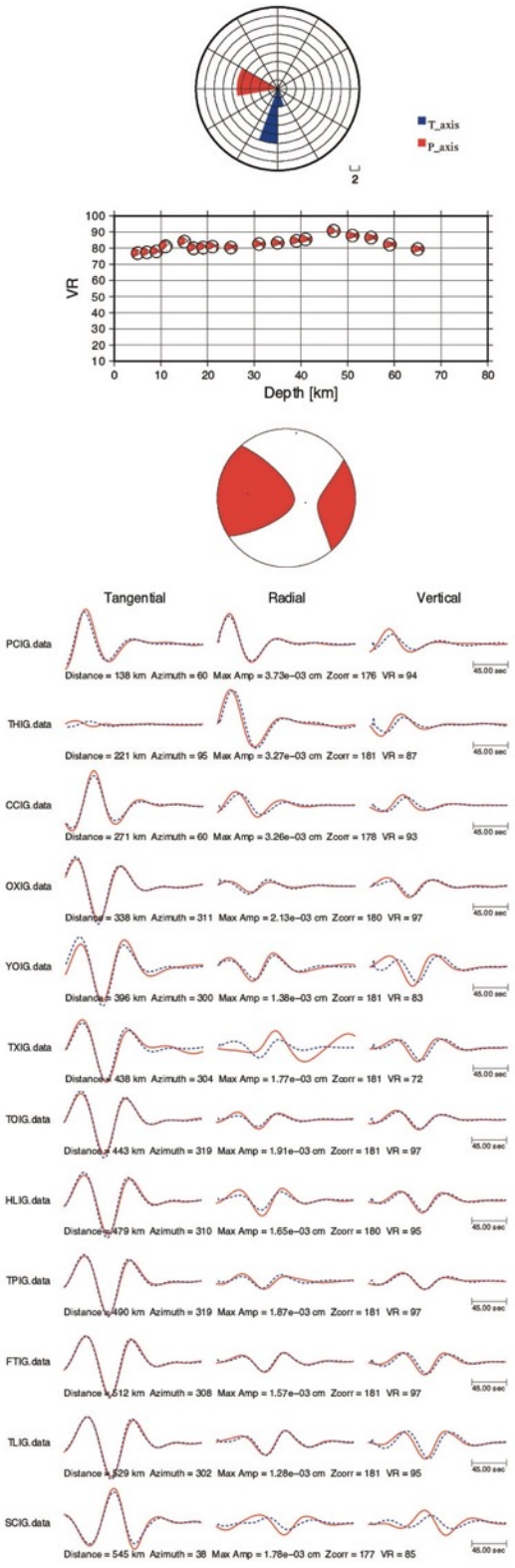

Figure S5. Moment tensor inversion of earthquake 4 (Table S1) after depth analysis. At the top we present the histogram of P and T axis. Middle. Variance Reduction (VR) as a function of depth. Bottom, time domain waveform inversion of the best solution.

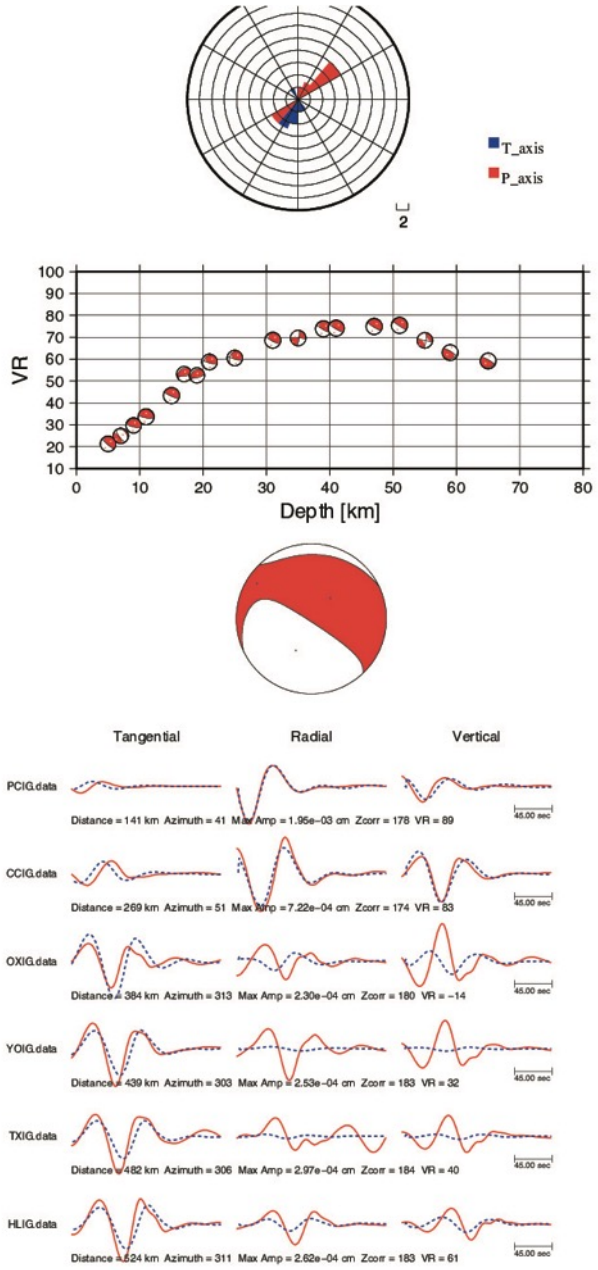

Figure S6. Moment tensor inversion of earthquake 5 (Table S1) after depth analysis. At the top we present the histogram of P and T axis. Middle. Variance Reduction (VR) as a function of depth. Bottom, time domain waveform inversion of the best solution.

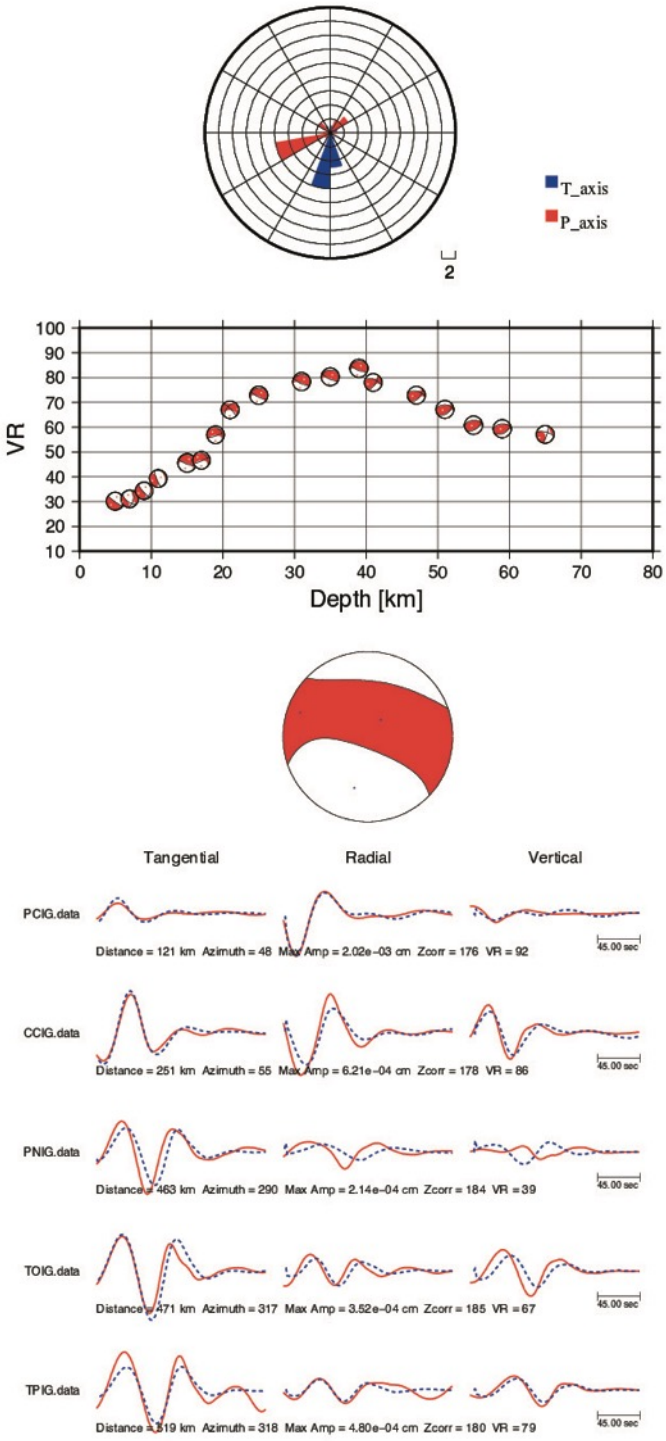

Figure S7. Moment tensor inversion of earthquake 6 (Table S1) after depth analysis. At the top we present the histogram of P and T axis. Middle. Variance Reduction (VR) as a function of depth. Bottom, time domain waveform inversion of the best solution.

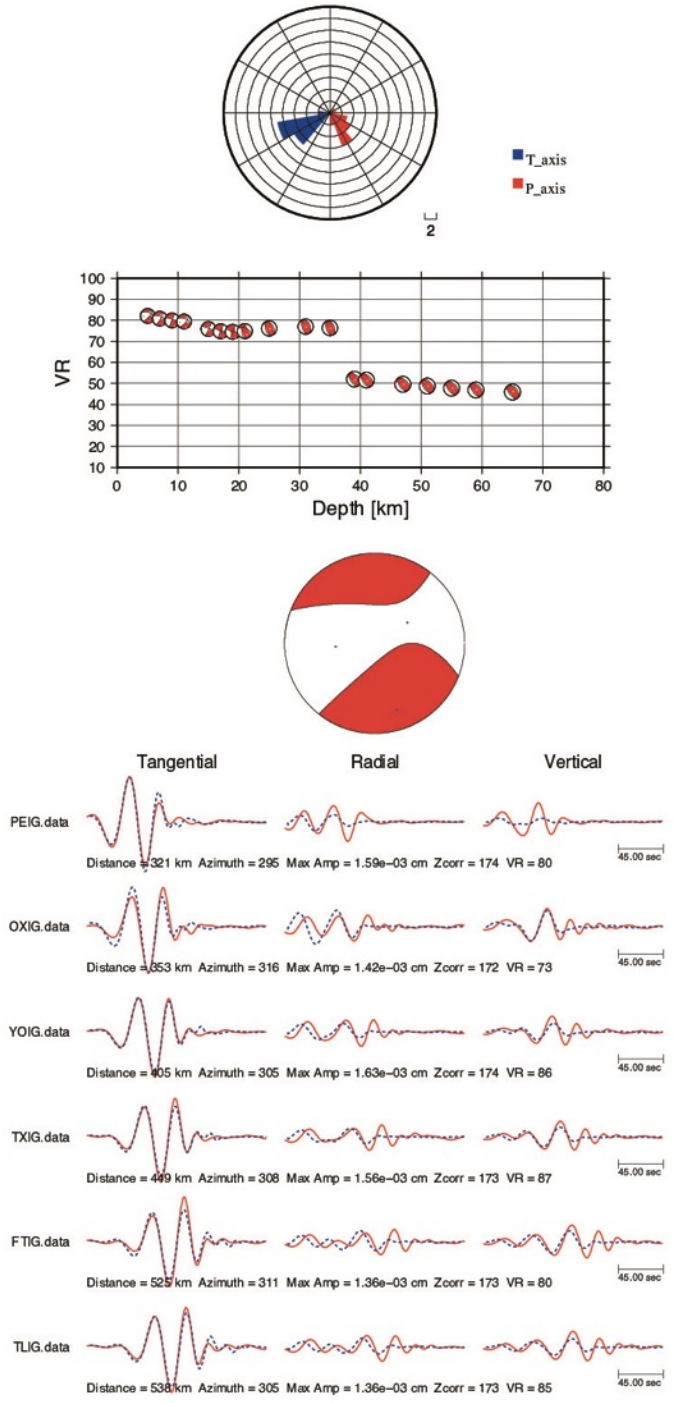

Figure S8. Moment tensor inversion of earthquake 7 (Table S1) after depth analysis. At the top we present the histogram of P and T axis. Middle. Variance Reduction (VR) as a function of depth. Bottom, time domain waveform inversion of the best solution.

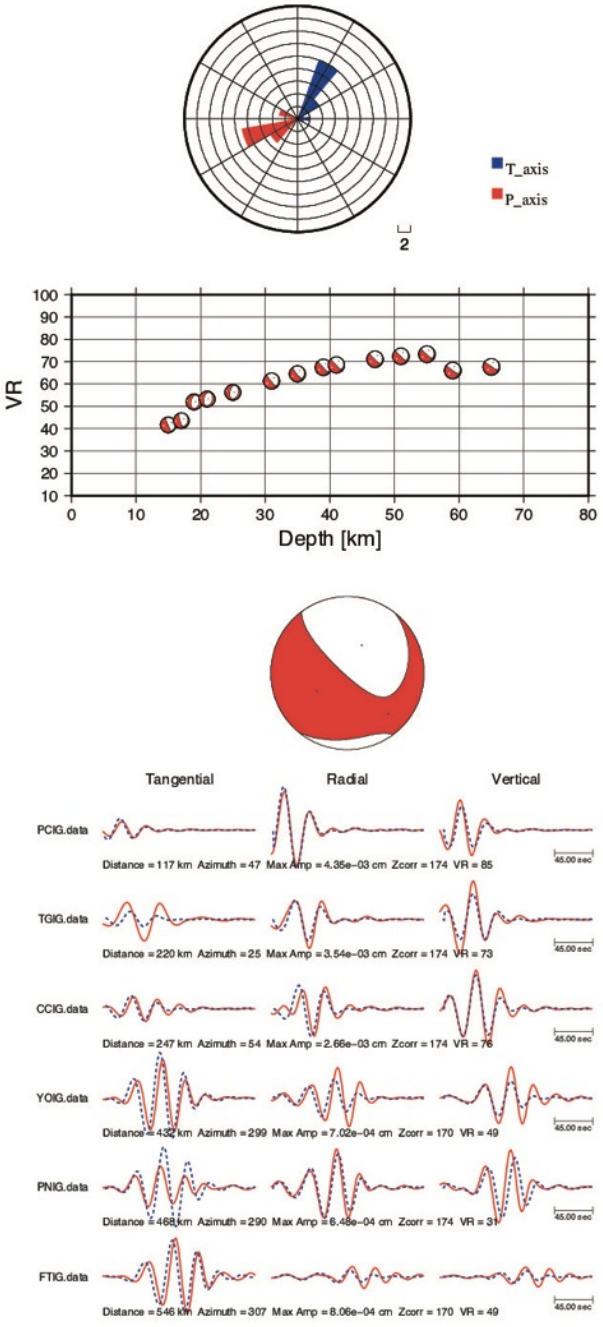

Figure S9. Moment tensor inversion of earthquake 8 (Table S1) after depth analysis. At the top we present the histogram of P and T axis. Middle. Variance Reduction (VR) as a function of depth. Bottom, time domain waveform inversion of the best solution.

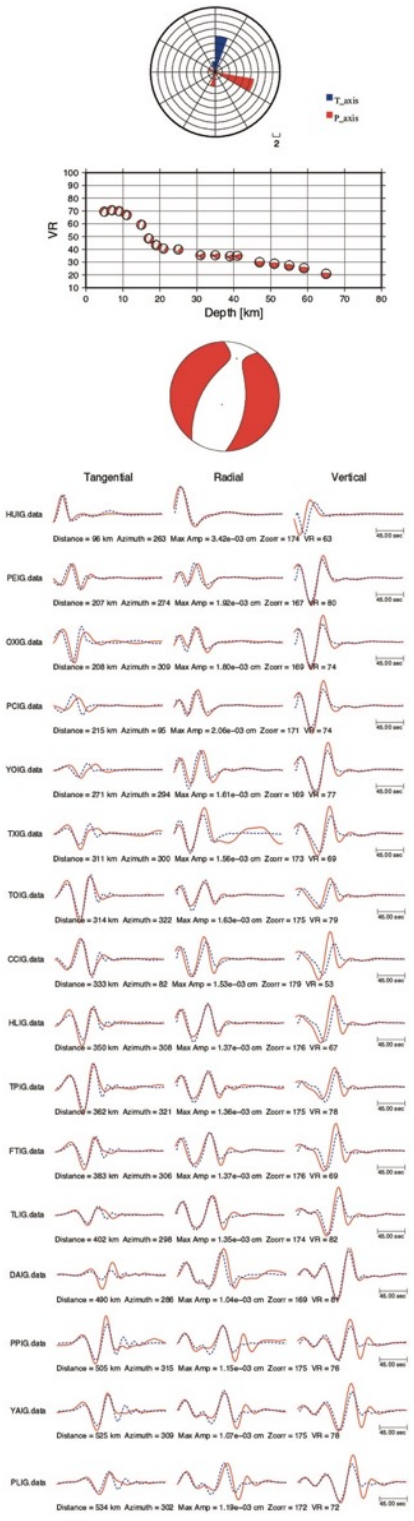

Figure S10. Moment tensor inversion of earthquake 9 (Table S1) after depth analysis. At the top we present the histogram of P and T axis. Middle. Variance Reduction (VR) as a function of depth. Bottom, time domain waveform inversion of the best solution.

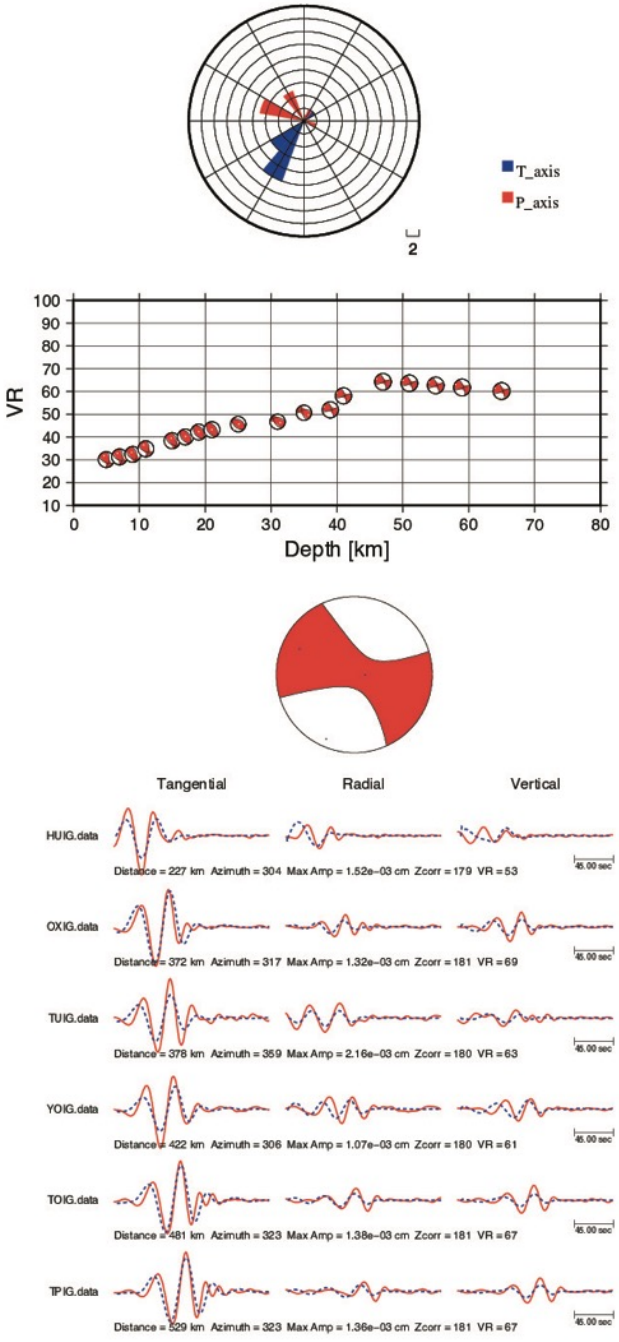

Figure S11. Moment tensor inversion of earthquake 10 (Table S1) after depth analysis. At the top we present the histogram of P and T axis. Middle. Variance Reduction (VR) as a function of depth. Bottom, time domain waveform inversion of the best solution.

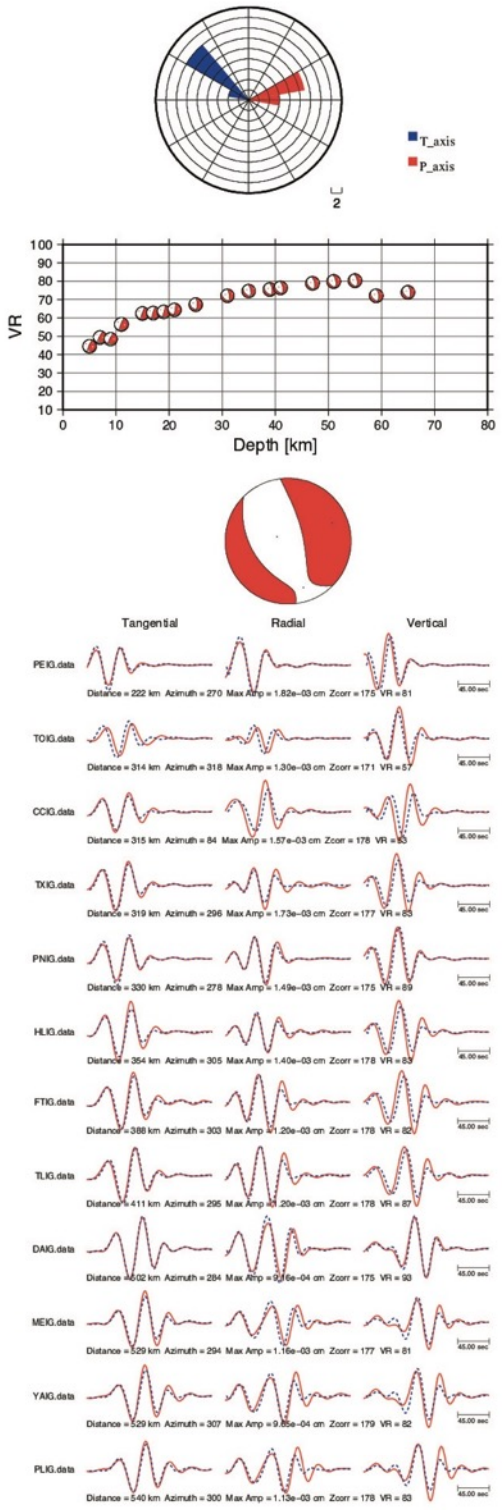

Figure S12. Moment tensor inversion of earthquake 11 (Table S1) after depth analysis. At the top we present the histogram of P and T axis. Middle. Variance Reduction (VR) as a function of depth. Bottom, time domain waveform inversion of the best solution.

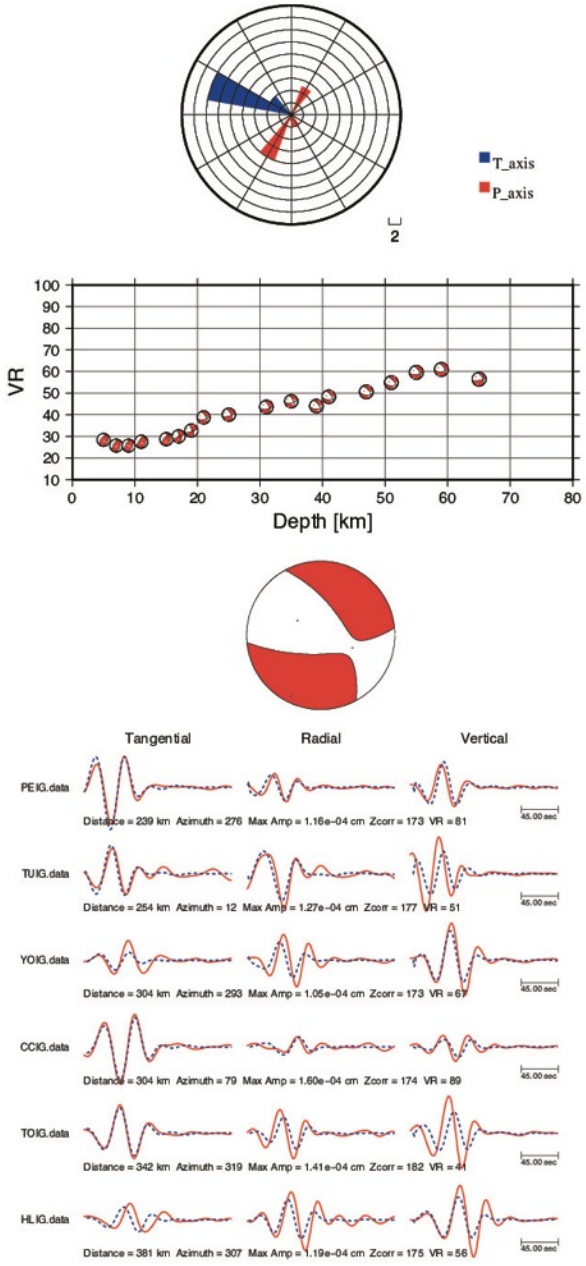

Figure S13. Moment tensor inversion of earthquake 12 (Table S1) after depth analysis. At the top we present the histogram of P and T axis. Middle. Variance Reduction (VR) as a function of depth. Bottom, time domain waveform inversion of the best solution.

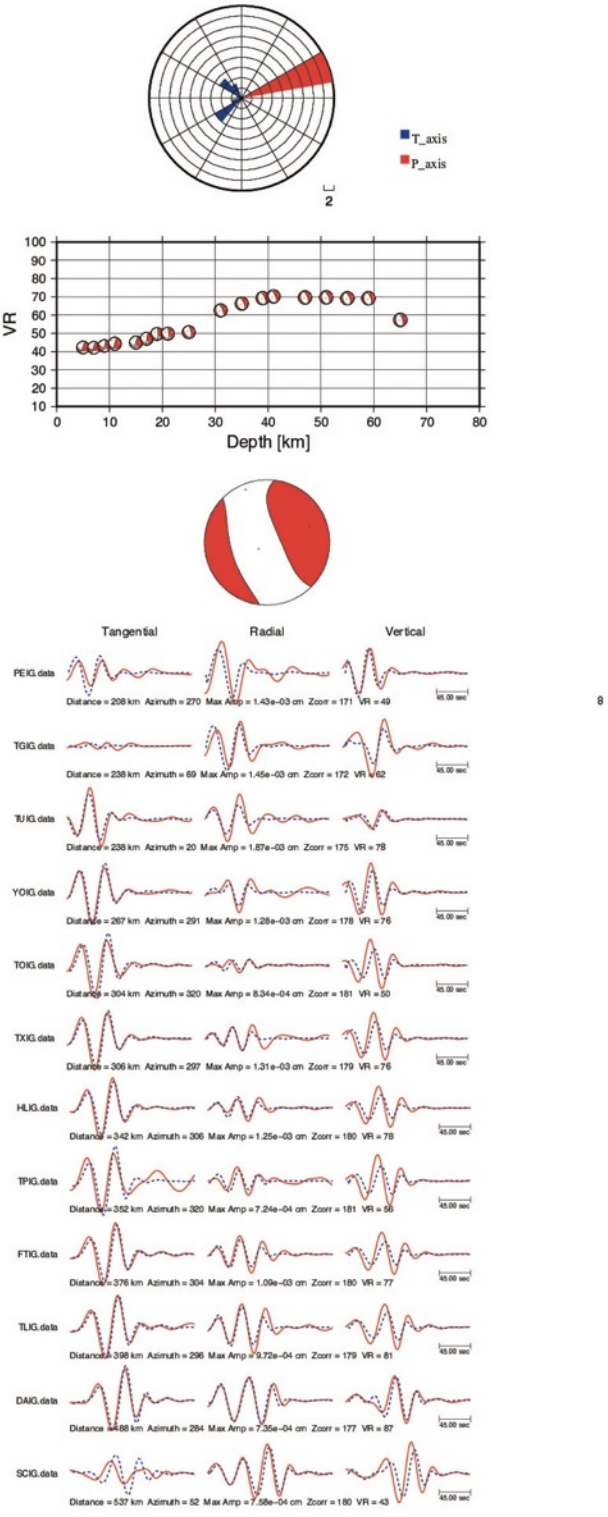

Figure S14. Moment tensor inversion of earthquake 13 (Table S1) after depth analysis. At the top we present the histogram of P and T axis. Middle. Variance Reduction (VR) as a function of depth. Bottom, time domain waveform inversion of the best solution.

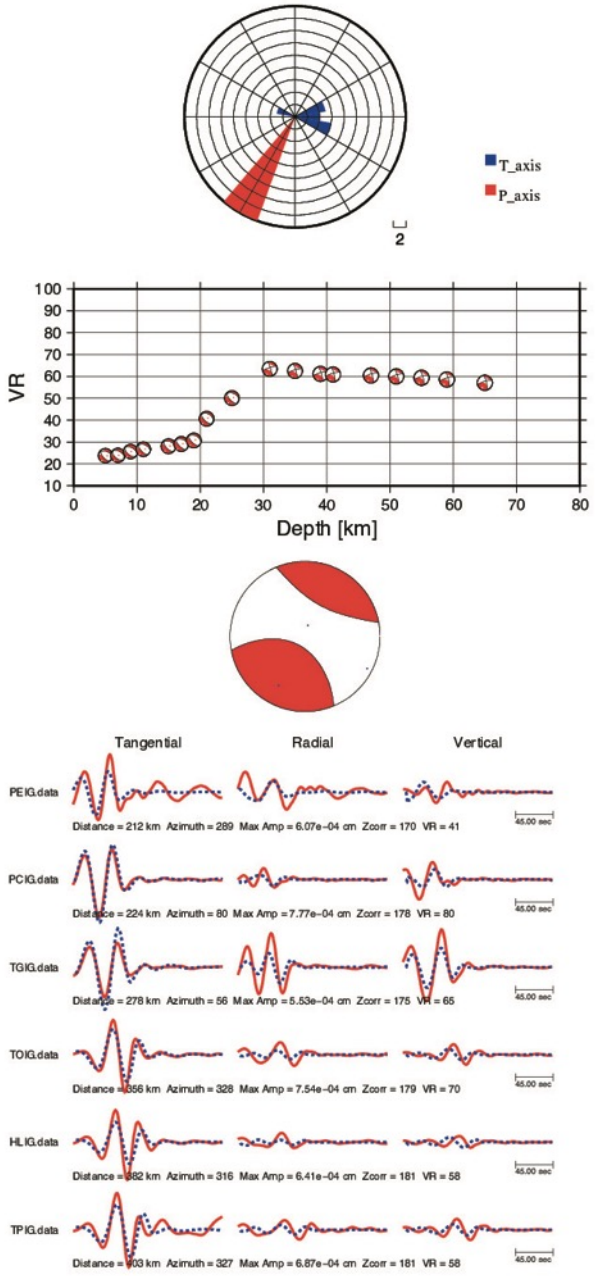

Figure S15. Moment tensor inversion of earthquake 14 (Table S1) after depth analysis. At the top we present the histogram of P and T axis. Middle. Variance Reduction (VR) as a function of depth. Bottom, time domain waveform inversion of the best solution.

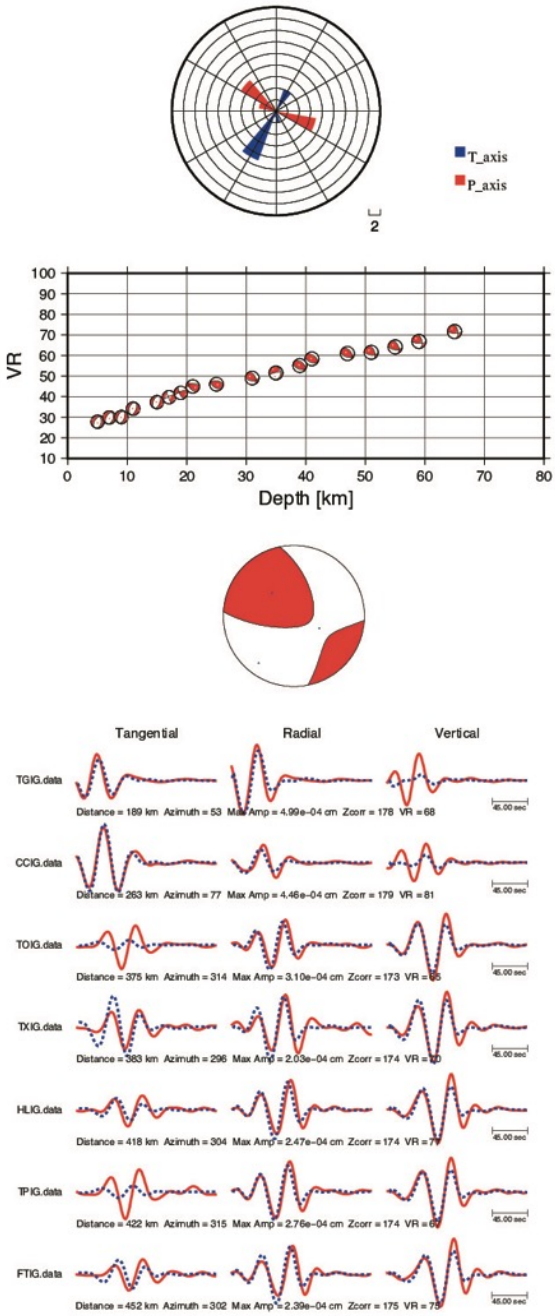

Figure S16. Moment tensor inversion of earthquake 15 (Table S1) after depth analysis. At the top we present the histogram of P and T axis. Middle. Variance Reduction (VR) as a function of depth. Bottom, time domain waveform inversion of the best solution.

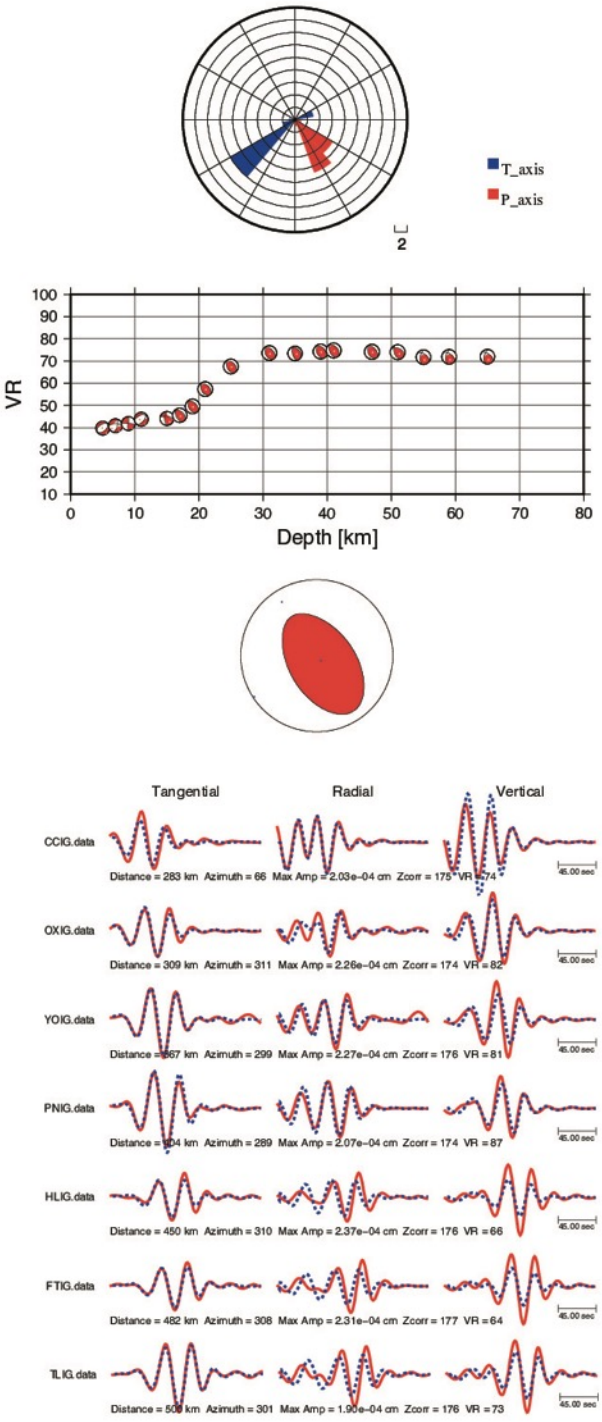

Figure S17. Moment tensor inversion of earthquake 16 (Table S1) after depth analysis. At the top we present the histogram of P and T axis. Middle. Variance Reduction (VR) as a function of depth. Bottom, time domain waveform inversion of the best solution.

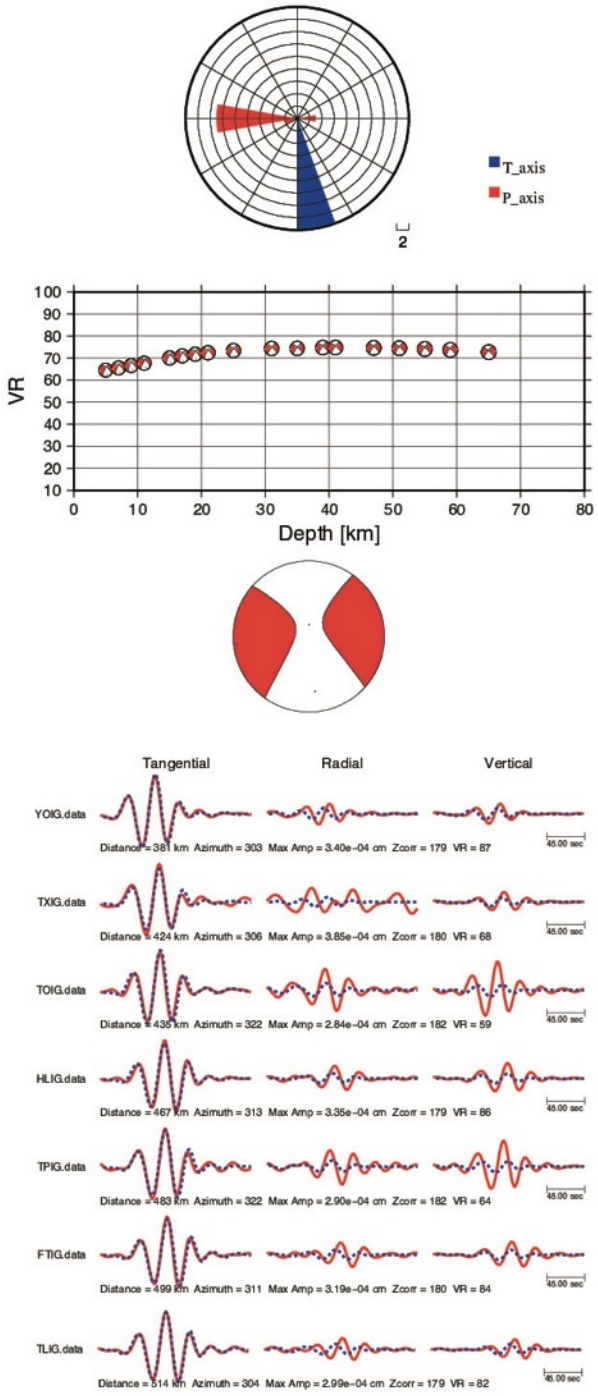

Figure S18. Moment tensor inversion of earthquake 17 (Table S1) after depth analysis. At the top we present the histogram of P and T axis. Middle. Variance Reduction (VR) as a function of depth. Bottom, time domain waveform inversion of the best solution.

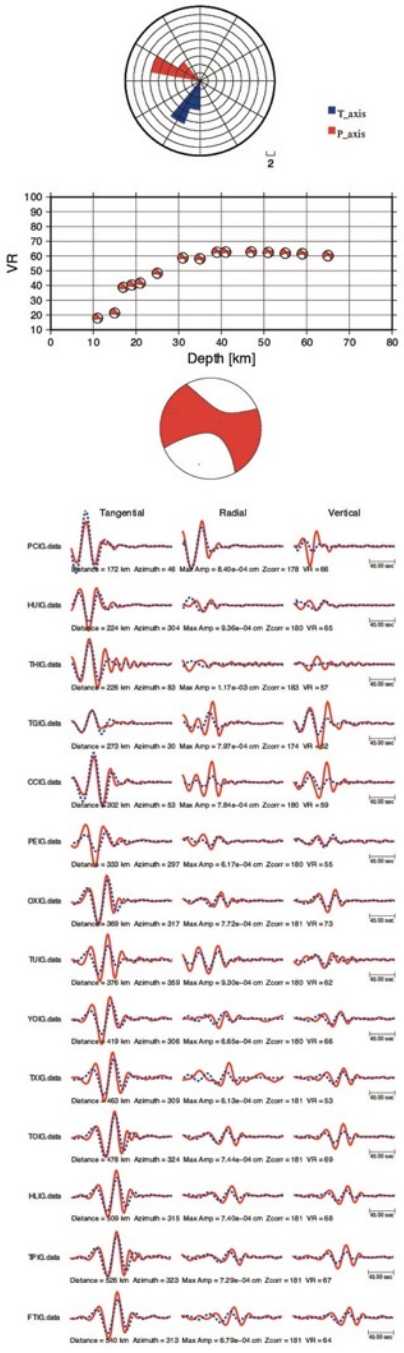

Figure S19. Moment tensor inversion of earthquake 18 (Table S1) after depth analysis. At the top we present the histogram of P and T axis. Middle. Variance Reduction (VR) as a function of depth. Bottom, time domain waveform inversion of the best solution.

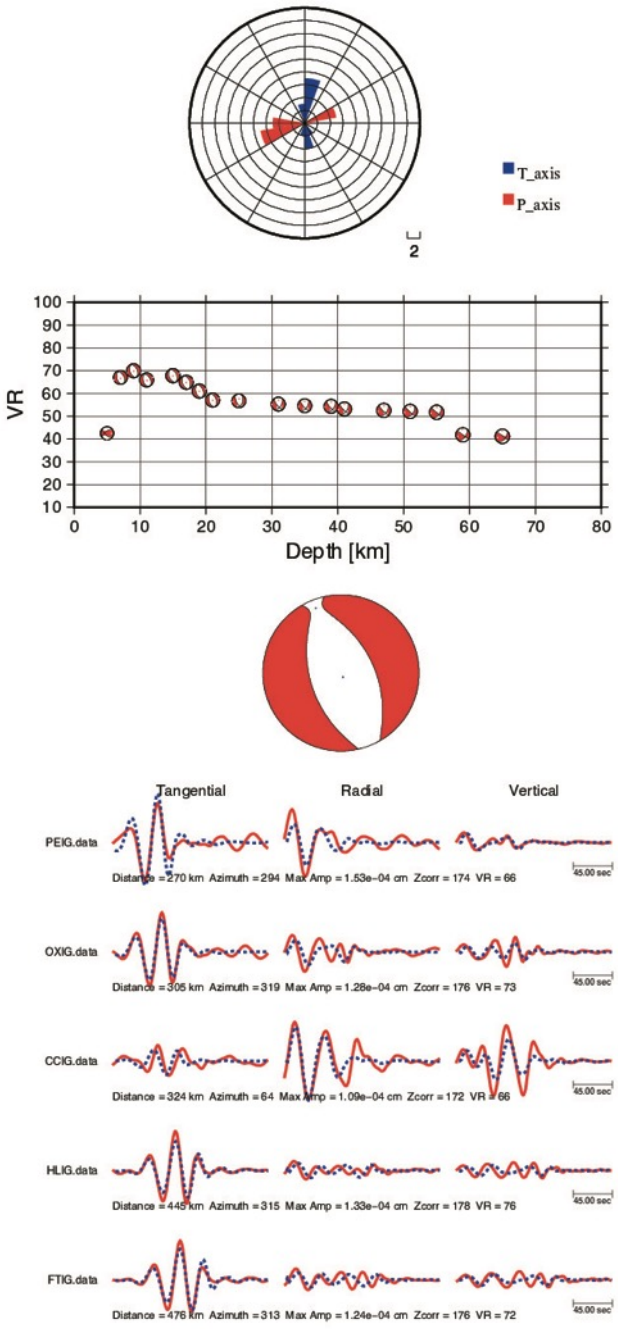

Figure S20. Moment tensor inversion of earthquake 19 (Table S1) after depth analysis. At the top we present the histogram of P and T axis. Middle. Variance Reduction (VR) as a function of depth. Bottom, time domain waveform inversion of the best solution.

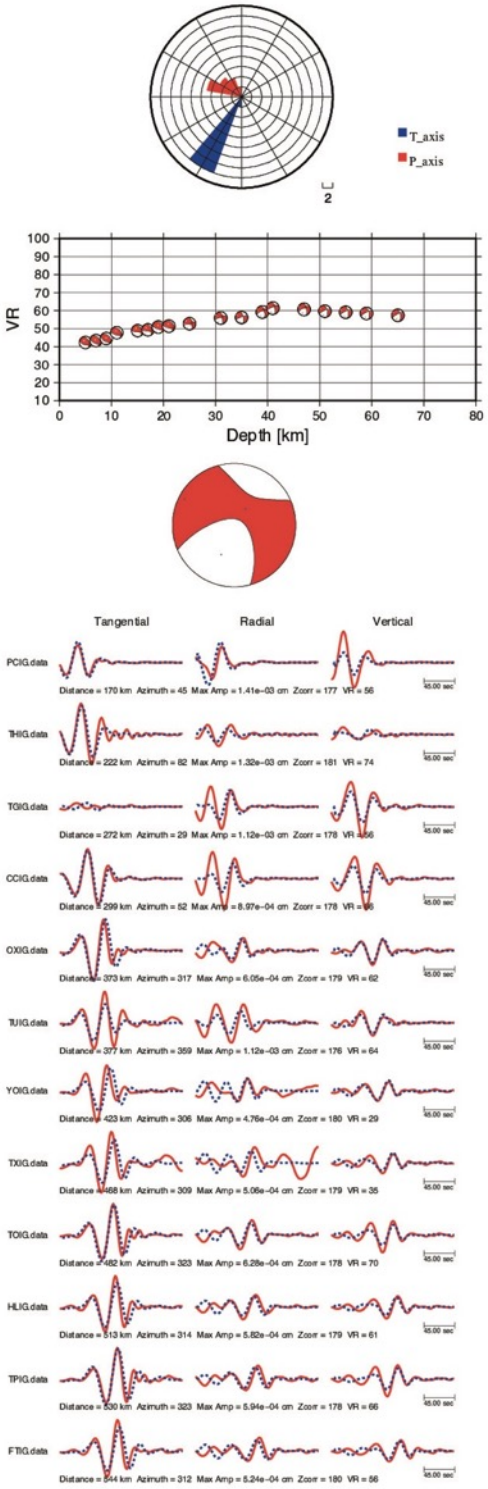

Figure S21. Moment tensor inversion of earthquake 20(Table S1) after depth analysis. At the top we present the histogram of P and T axis. Middle. Variance Reduction (VR) as a function of depth. Bottom, time domain waveform inversion of the best solution.

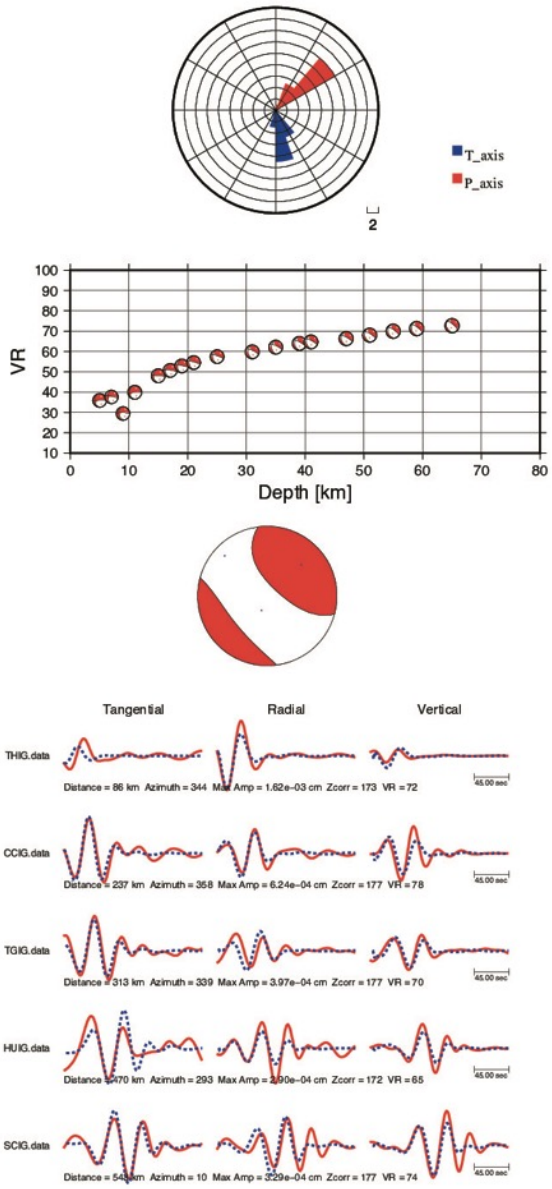

Figure S22. Moment tensor inversion of earthquake 21 (Table S1) after depth analysis. At the top we present the histogram of P and T axis. Middle. Variance Reduction (VR) as a function of depth. Bottom, time domain waveform inversion of the best solution.

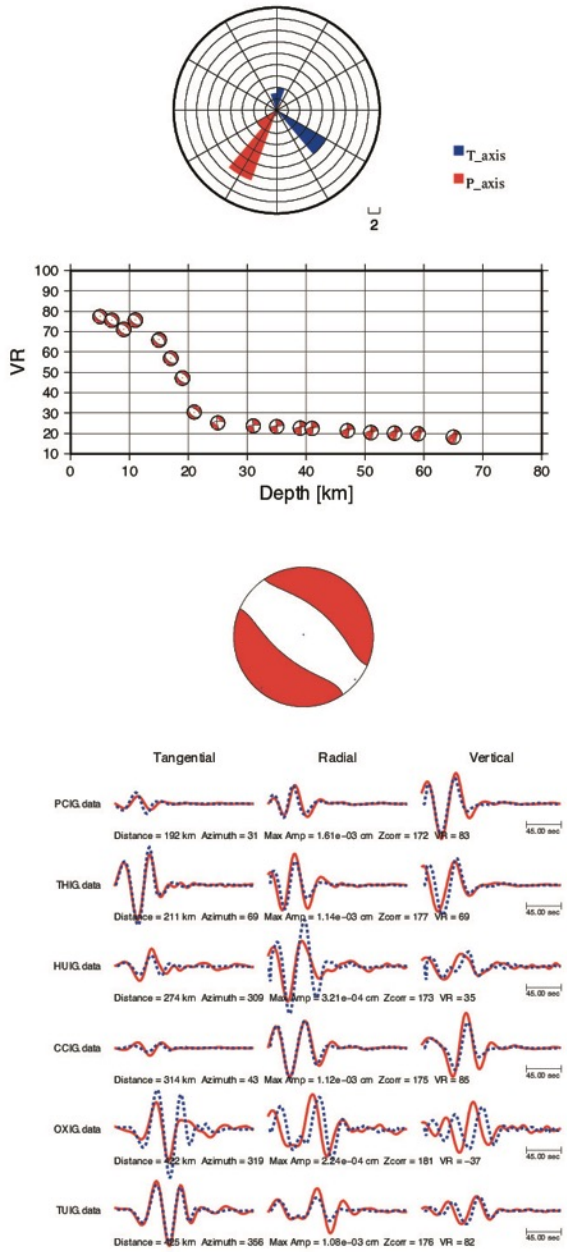

Figure S23. Moment tensor inversion of earthquake 22 (Table S1) after depth analysis. At the top we present the histogram of P and T axis. Middle. Variance Reduction (VR) as a function of depth. Bottom, time domain waveform inversion of the best solution.

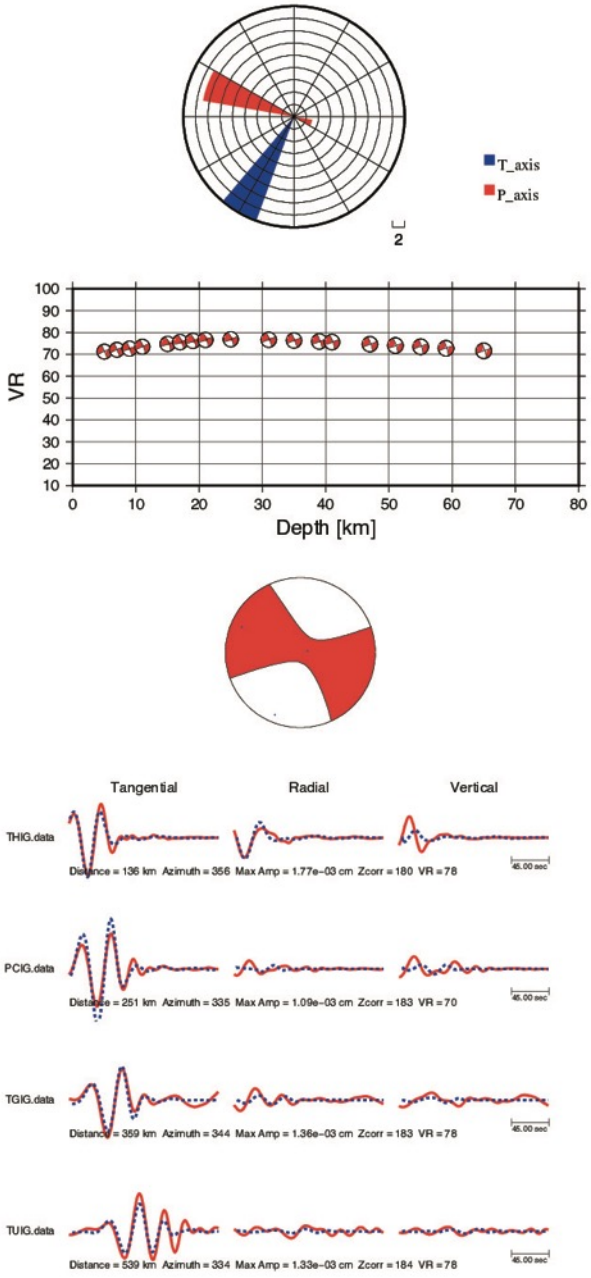

Figure S24. Moment tensor inversion of earthquake 23 (Table S1) after depth analysis. At the top we present the histogram of P and T axis. Middle. Variance Reduction (VR) as a function of depth. Bottom, time domain waveform inversion of the best solution.

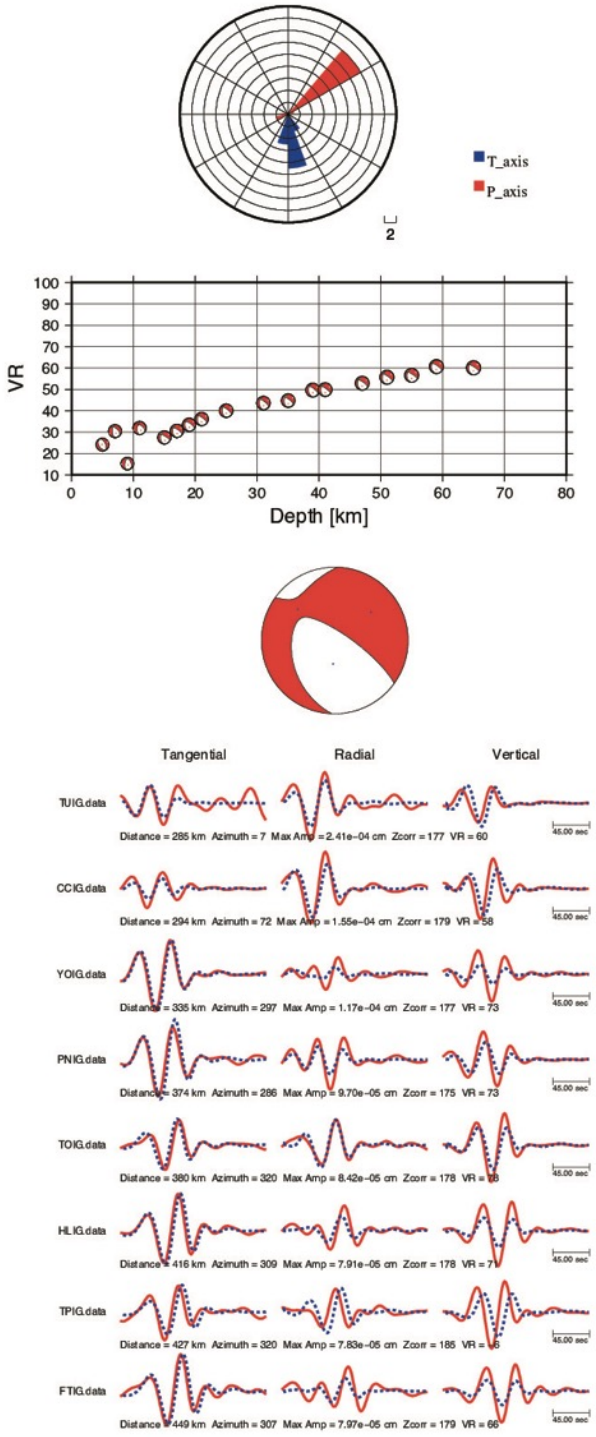

Figure S25. Moment tensor inversion of earthquake 24 (Table S1) after depth analysis. At the top we present the histogram of P and T axis. Middle. Variance Reduction (VR) as a function of depth. Bottom, time domain waveform inversion of the best solution.

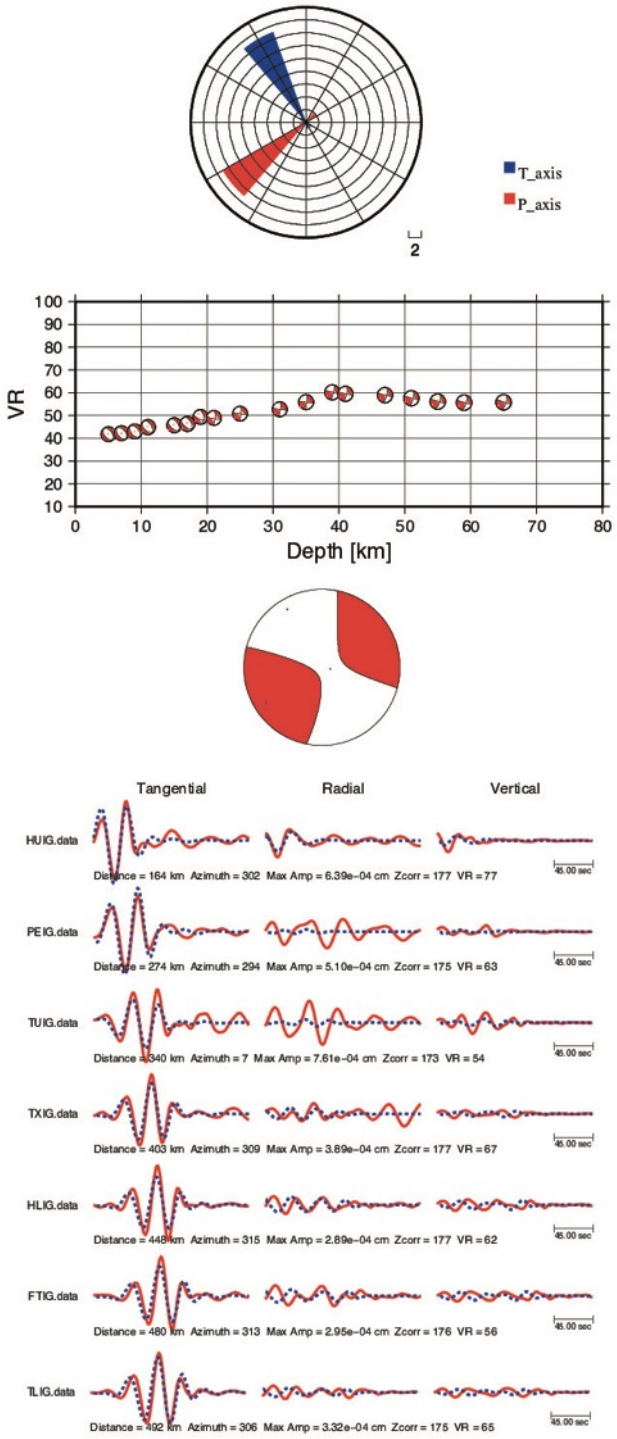

Figure S26. Moment tensor inversion of earthquake 25 (Table S1) after depth analysis. At the top we present the histogram of P and T axis. Middle. Variance Reduction (VR) as a function of depth. Bottom, time domain waveform inversion of the best solution

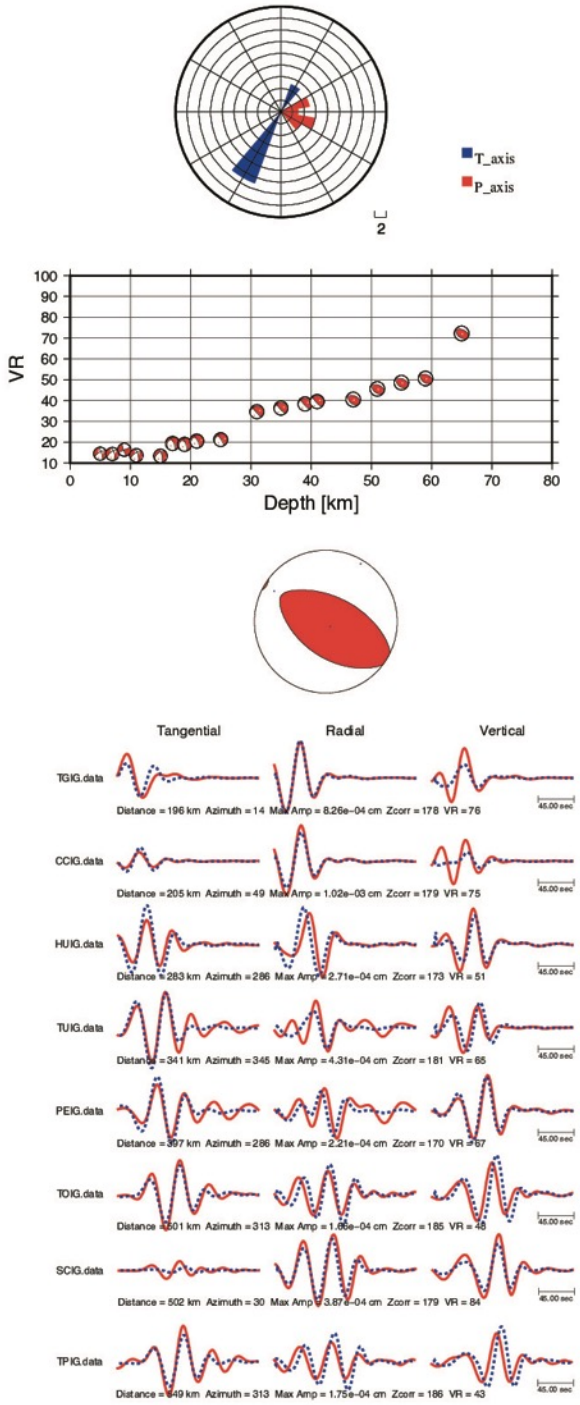

Figure S27. Moment tensor inversion of earthquake 26 (Table S1) after depth analysis. At the top we present the histogram of P and T axis. Middle. Variance Reduction (VR) as a function of depth. Bottom, time domain waveform inversion of the best solution

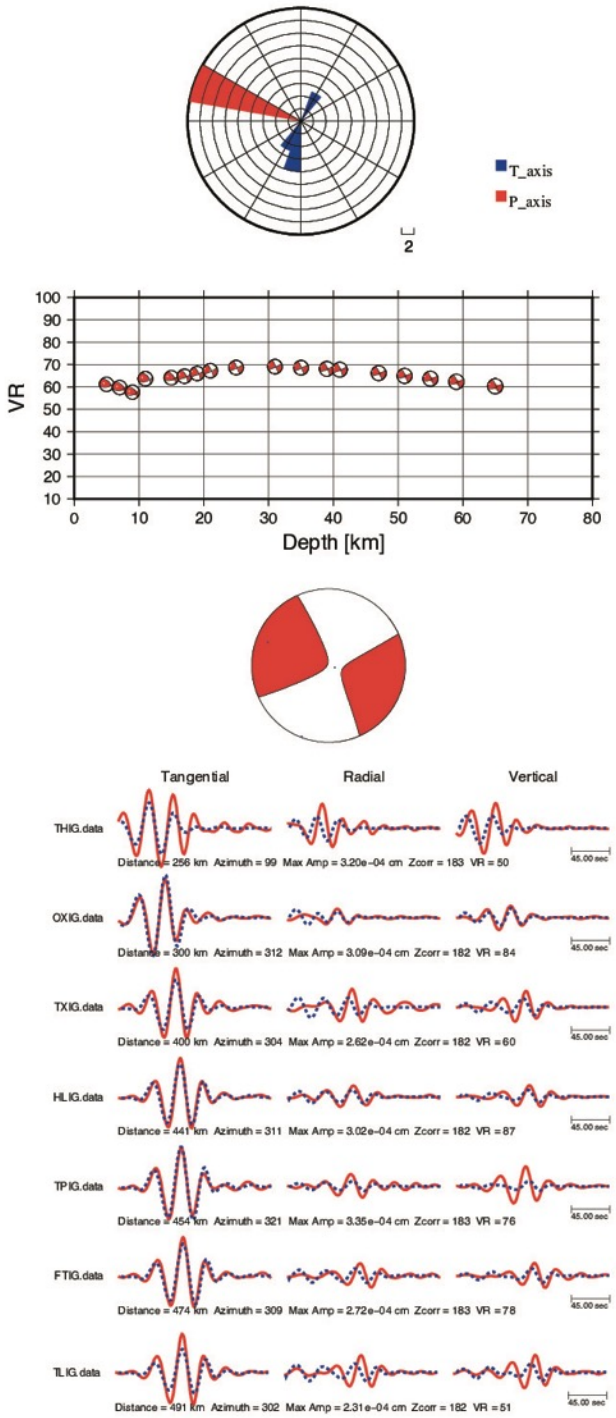

Figure S28. Moment tensor inversion of earthquake 27 (Table S1) after depth analysis. At the top we present the histogram of P and T axis. Middle. Variance Reduction (VR) as a function of depth. Bottom, time domain waveform inversion of the best solution

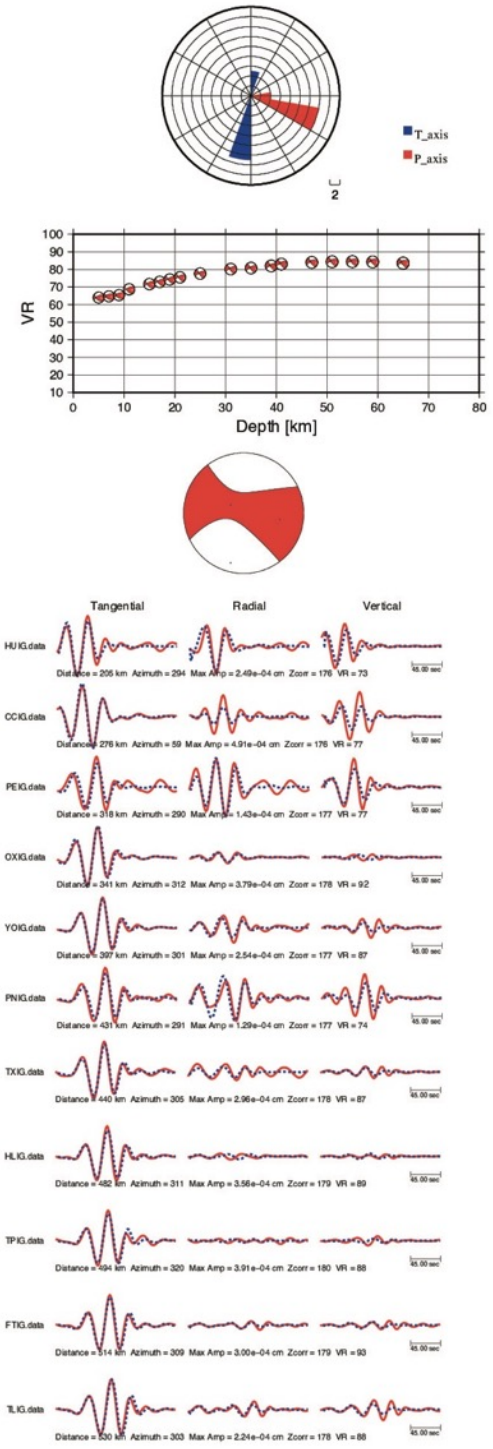

Figure S29. Moment tensor inversion of earthquake 28 (Table S1) after depth analysis. At the top we present the histogram of P and T axis. Middle. Variance Reduction (VR) as a function of depth. Bottom, time domain waveform inversion of the best solution

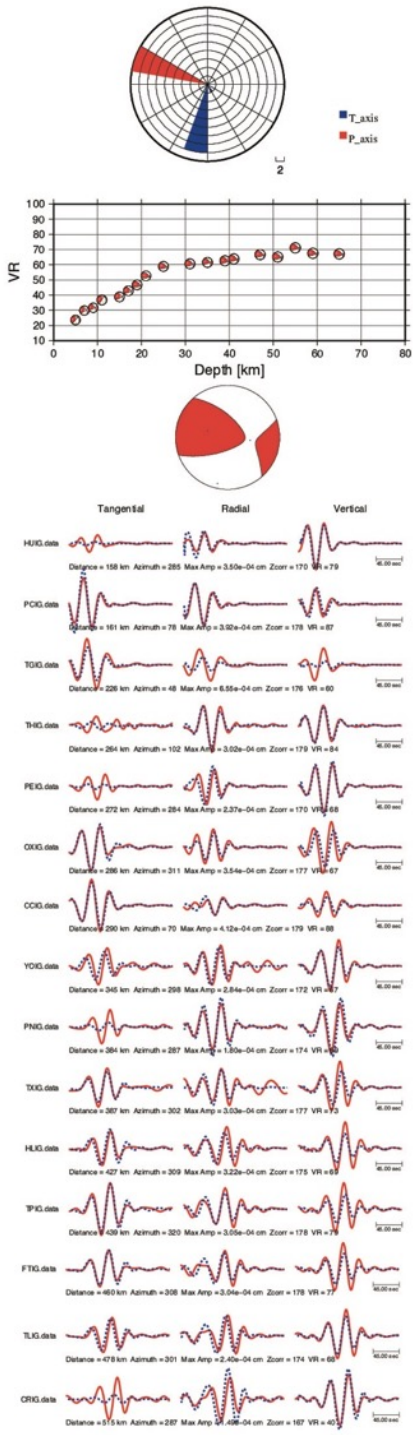

Figure S30. Moment tensor inversion of earthquake 29 (Table S1) after depth analysis. At the top we present the histogram of P and T axis. Middle. Variance Reduction (VR) as a function of depth. Bottom, time domain waveform inversion of the best solution

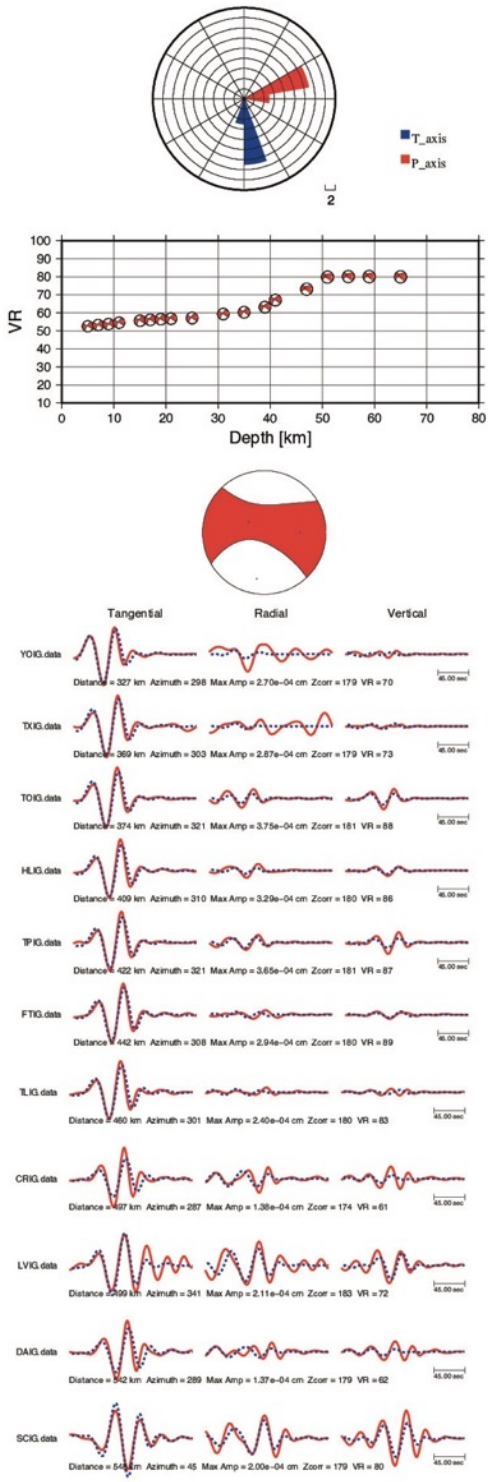

Figure S31. Moment tensor inversion of earthquake 30 (Table S1) after depth analysis. At the top we present the histogram of P and T axis. Middle. Variance Reduction (VR) as a function of depth. Bottom, time domain waveform inversion of the best solution

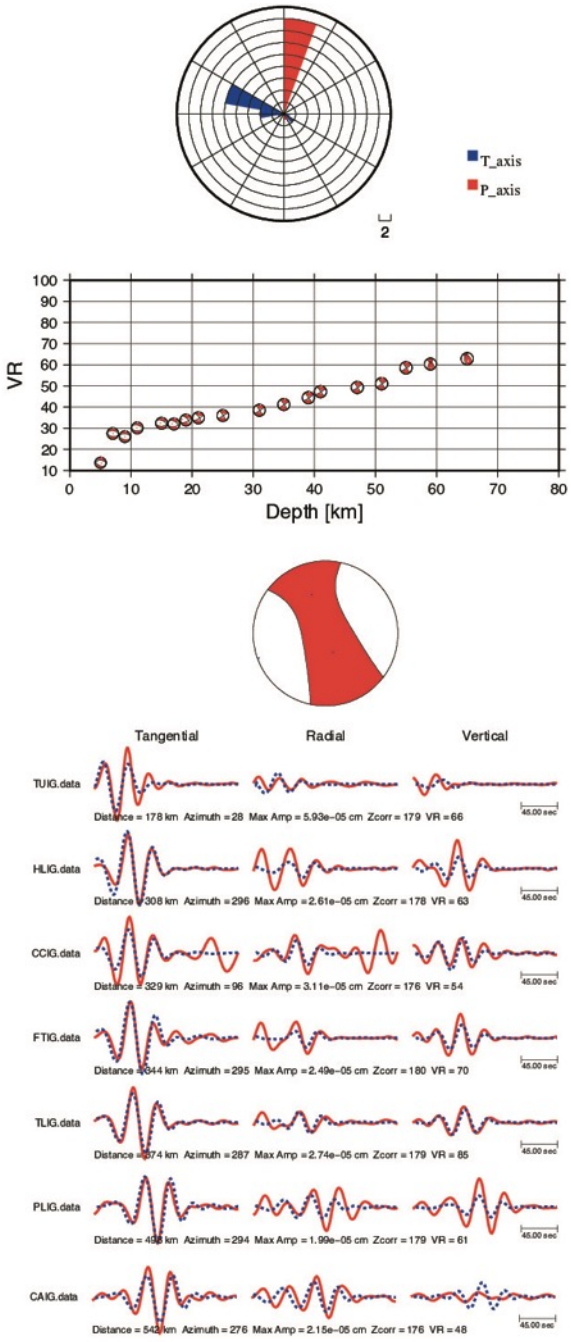

Figure S32. Moment tensor inversion of earthquake 31 (Table S1) after depth analysis. At the top we present the histogram of P and T axis. Middle. Variance Reduction (VR) as a function of depth. Bottom, time domain waveform inversion of the best solution

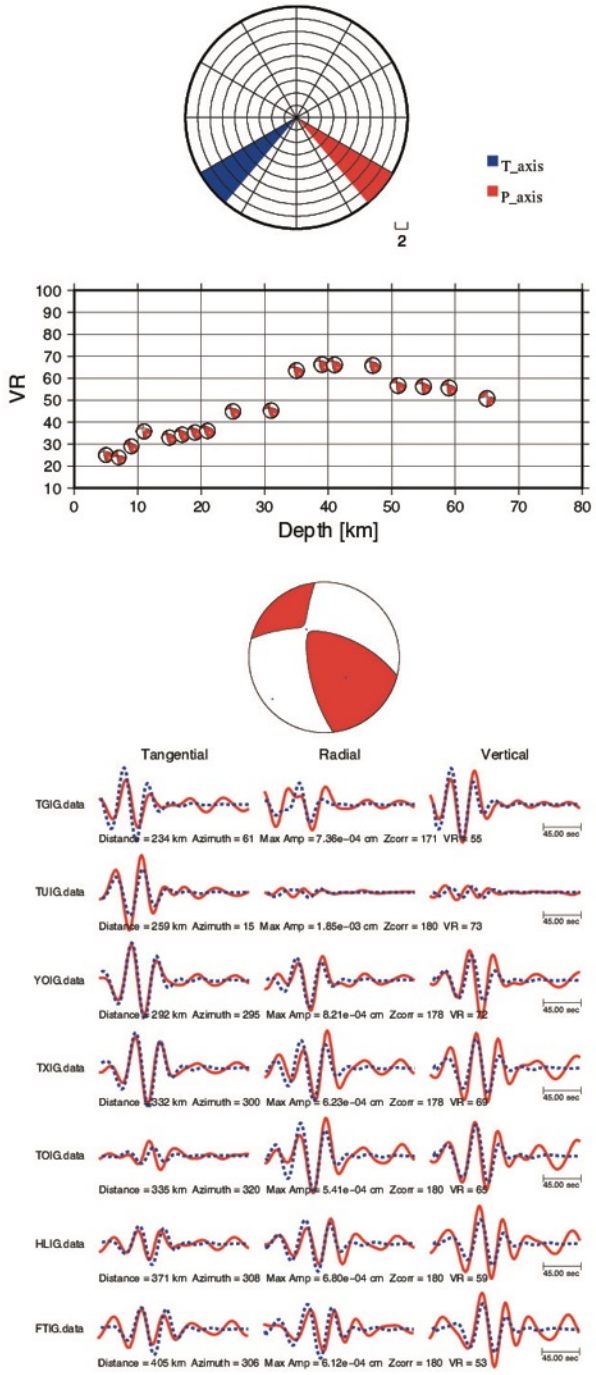

Figure S33. Moment tensor inversion of earthquake 32 (Table S1) after depth analysis. At the top we present the histogram of P and T axis. Middle. Variance Reduction (VR) as a function of depth. Bottom, time domain waveform inversion of the best solution

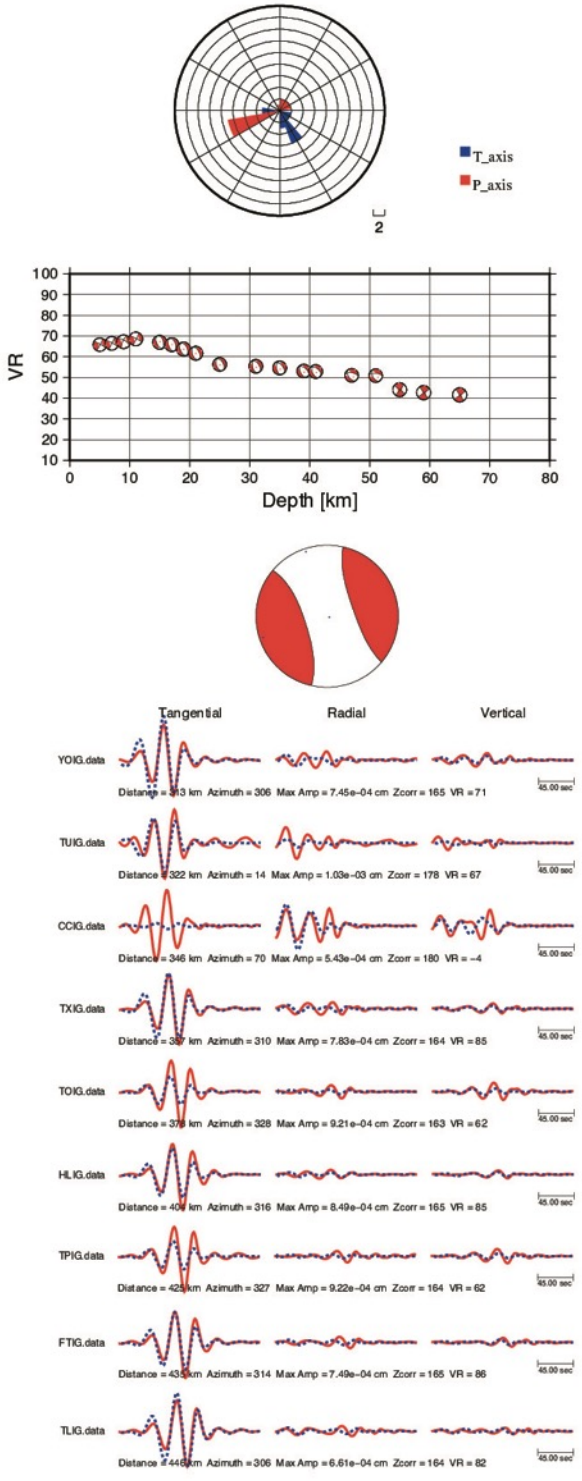

Figure S34. Moment tensor inversion of earthquake 33 (Table S1) after depth analysis. At the top we present the histogram of P and T axis. Middle. Variance Reduction (VR) as a function of depth. Bottom, time domain waveform inversion of the best solution

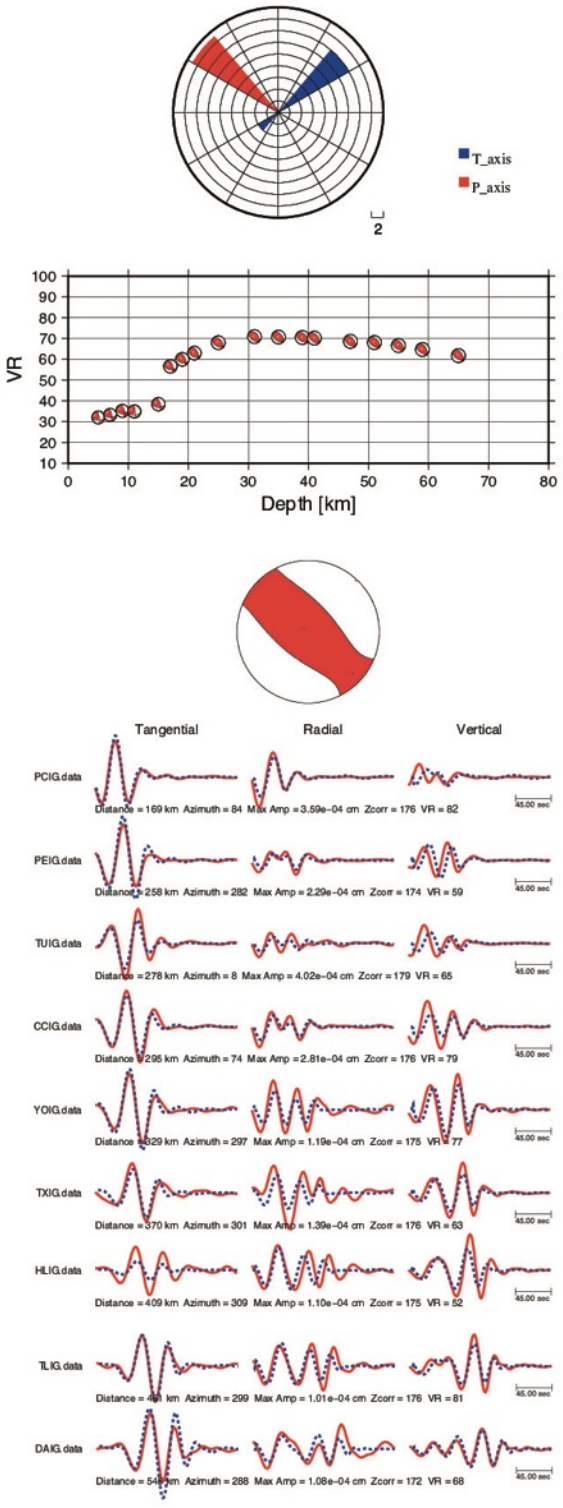

Figure S35. Moment tensor inversion of earthquake 34 (Table S1) after depth analysis. At the top we present the histogram of P and T axis. Middle. Variance Reduction (VR) as a function of depth. Bottom, time domain waveform inversion of the best solution

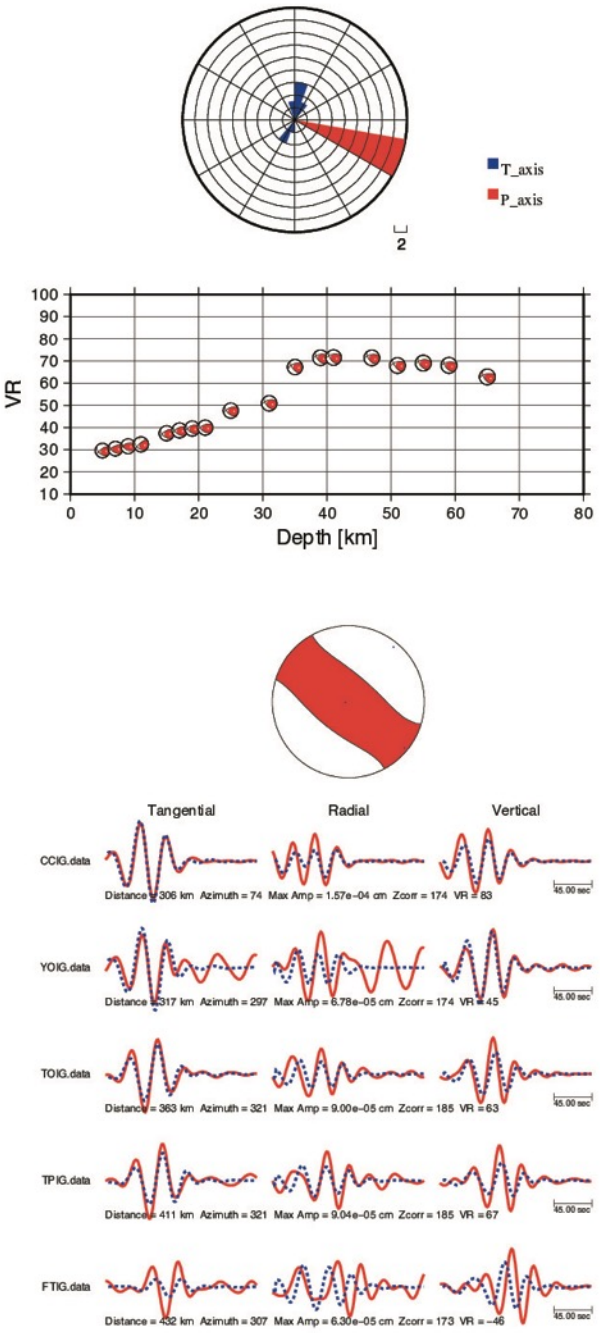

Figure S36. Moment tensor inversion of earthquake 35 (Table S1) after depth analysis. At the top we present the histogram of P and T axis. Middle. Variance Reduction (VR) as a function of depth. Bottom, time domain waveform inversion of the best solution

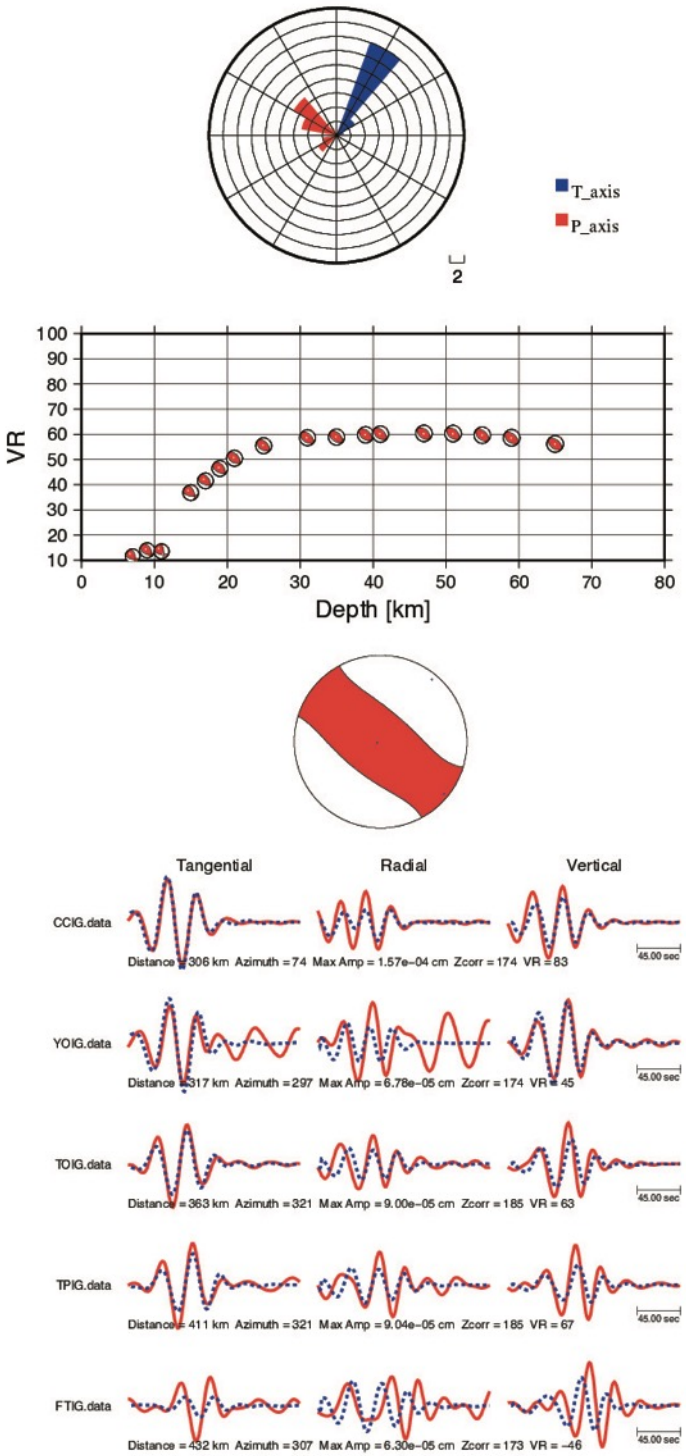

Figure S37. Moment tensor inversion of earthquake 36 (Table S1) after depth analysis. At the top we present the histogram of P and T axis. Middle. Variance Reduction (VR) as a function of depth. Bottom, time domain waveform inversion of the best solution

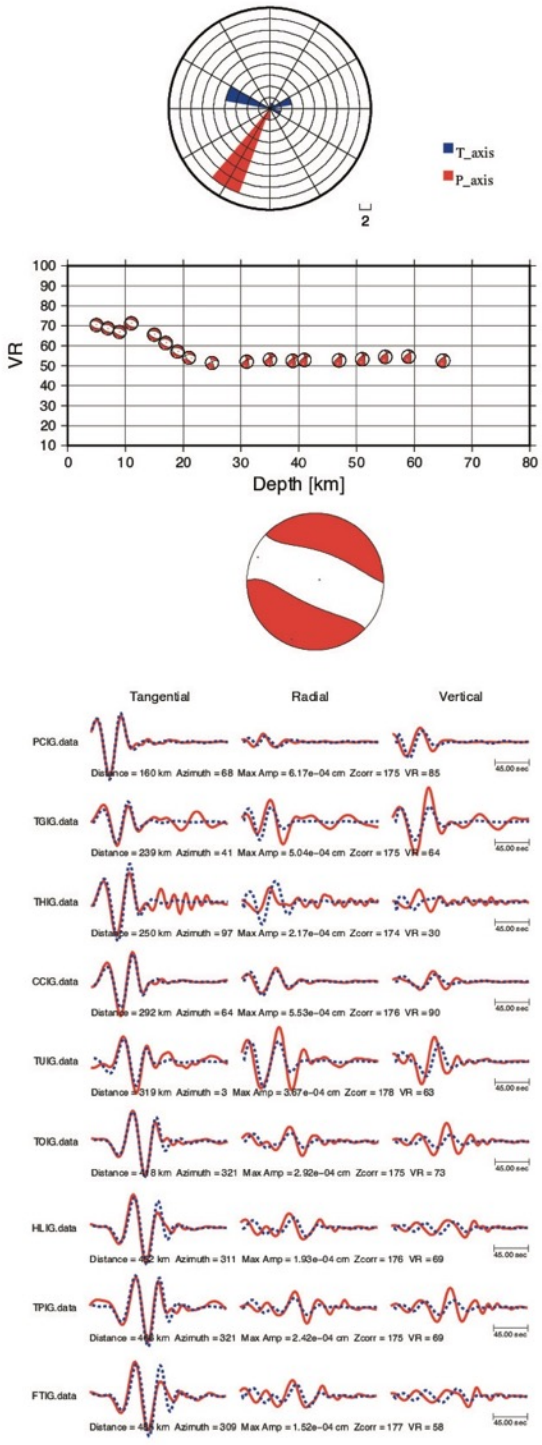

Figure 38. Moment tensor inversion of earthquake 37 (Table S1) after depth analysis. At the top we present the histogram of P and T axis. Middle. Variance Reduction (VR) as a function of depth. Bottom, time domain waveform inversion of the best solution

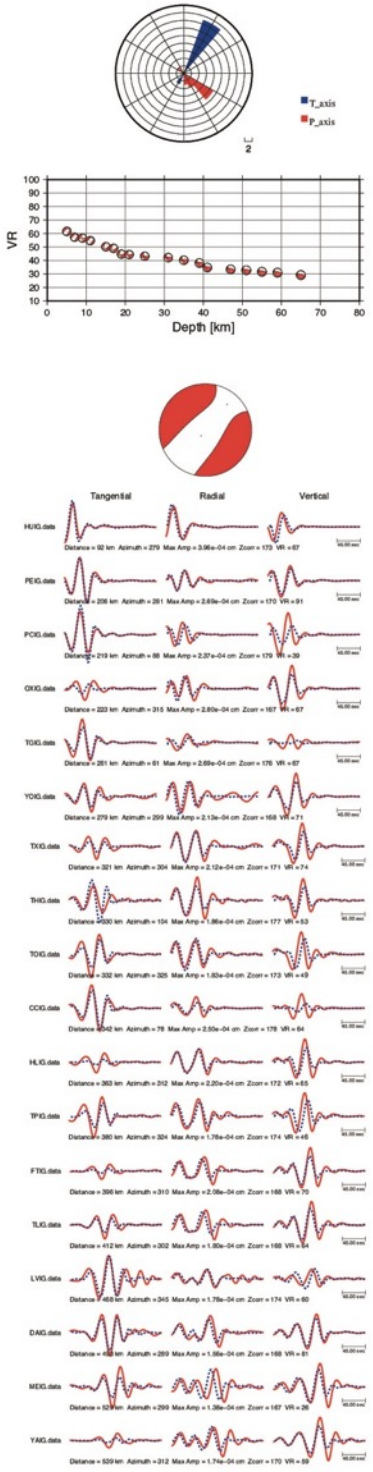

Figure S39. Moment tensor inversion of earthquake 38 (Table S1) after depth analysis. At the top we present the histogram of P and T axis. Middle. Variance Reduction (VR) as a function of depth. Bottom, time domain waveform inversion of the best solution

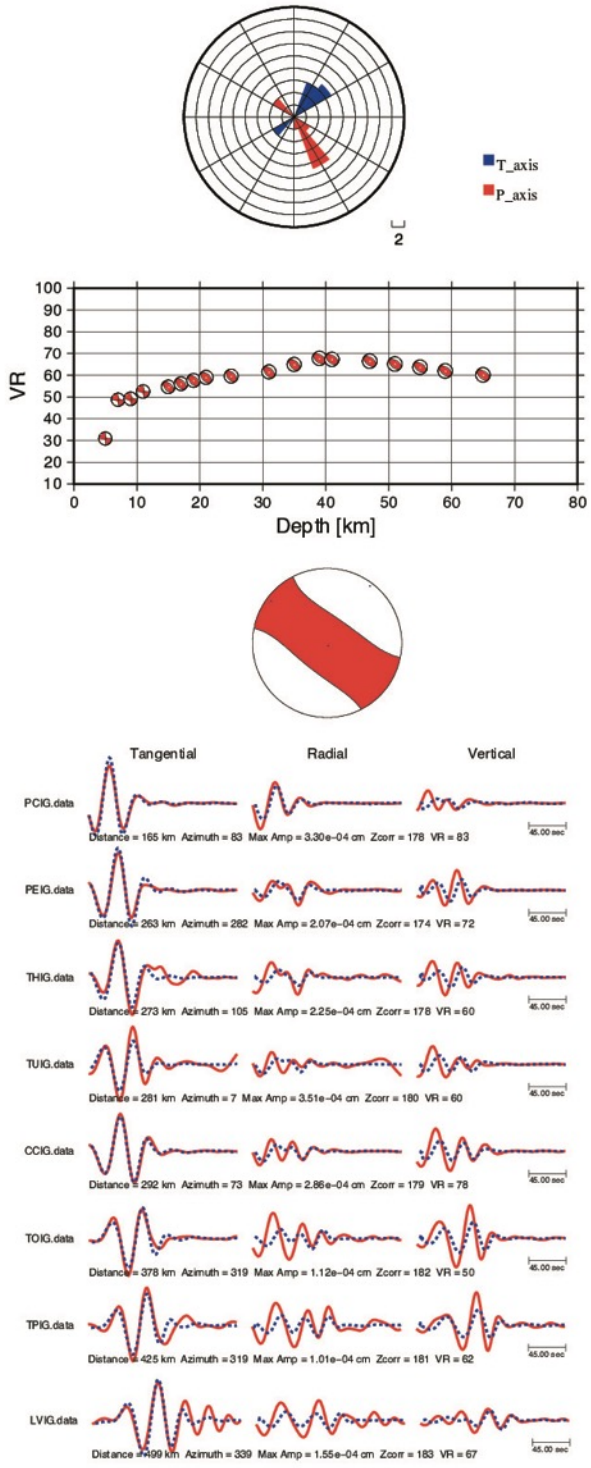

Figure S40. Moment tensor inversion of earthquake 39 (Table S1) after depth analysis. At the top we present the histogram of P and T axis. Middle. Variance Reduction (VR) as a function of depth. Bottom, time domain waveform inversion of the best solution

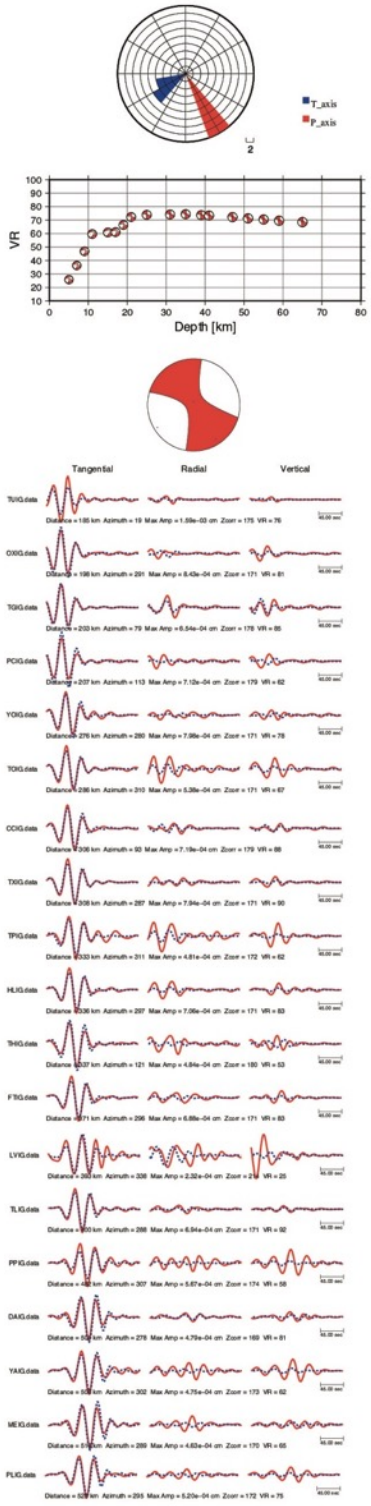

Figure S41. Moment tensor inversion of earthquake 40 (Table S1) after depth analysis. At the top we present the histogram of P and T axis. Middle. Variance Reduction (VR) as a function of depth. Bottom, time domain waveform inversion of the best solution

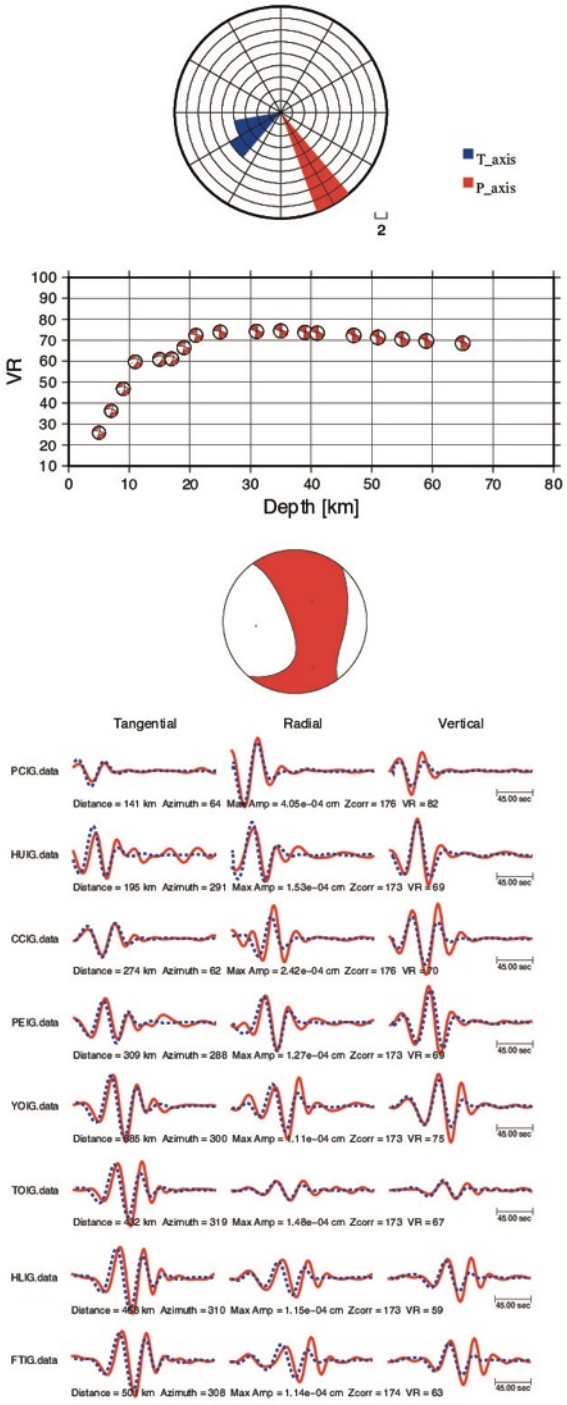

Figure S42. Moment tensor inversion of earthquake 41 (Table S1) after depth analysis. At the top we present the histogram of P and T axis. Middle. Variance Reduction (VR) as a function of depth. Bottom, time domain waveform inversion of the best solution

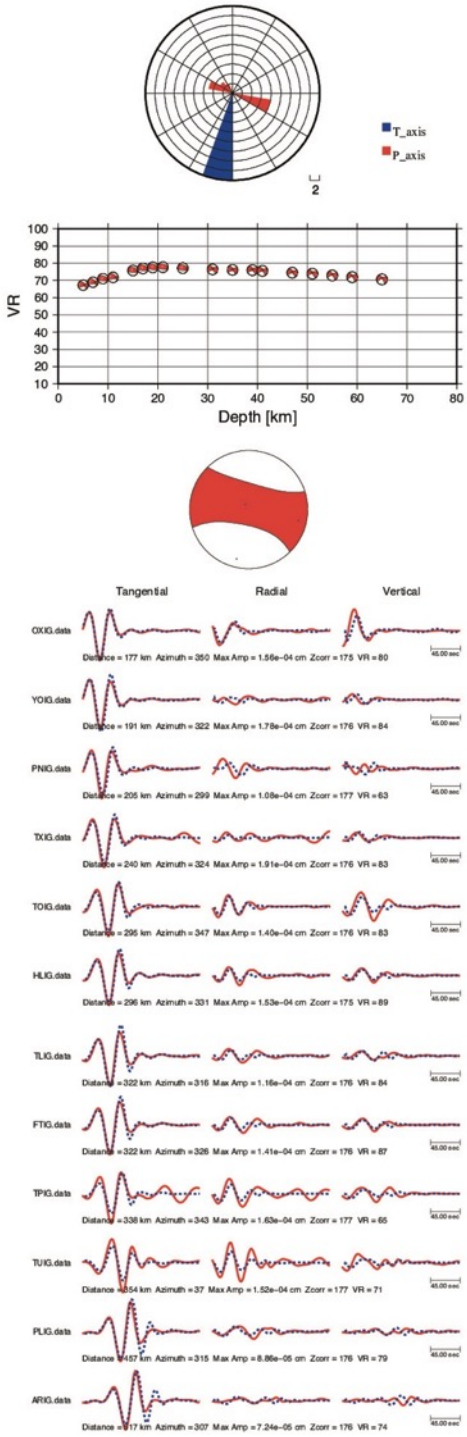

Figure S43. Moment tensor inversion of earthquake 42 (Table S1) after depth analysis. At the top we present the histogram of P and T axis. Middle. Variance Reduction (VR) as a function of depth. Bottom, time domain waveform inversion of the best solution

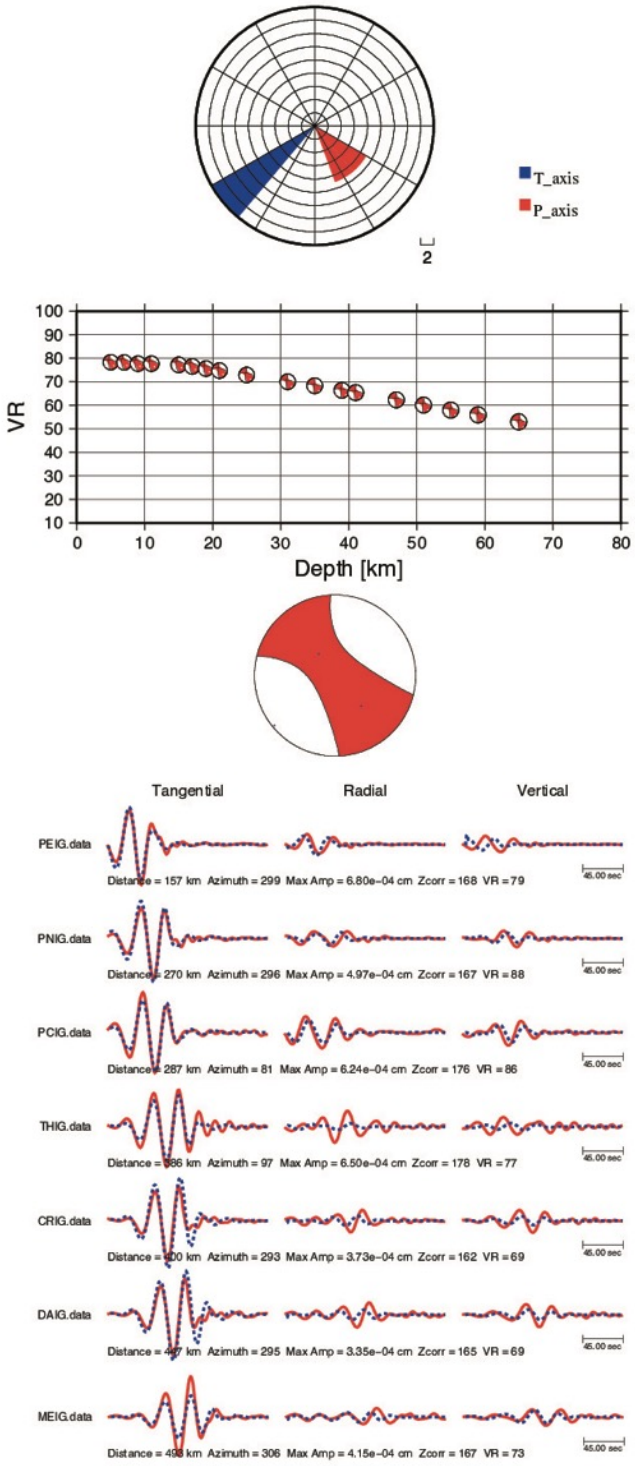

Figure S44. Moment tensor inversion of earthquake 43 (Table S1) after depth analysis. At the top we present the histogram of P and T axis. Middle. Variance Reduction (VR) as a function of depth. Bottom, time domain waveform inversion of the best solution